Analysis of Blockchain-based Smart Contracts for Peer-to-Peer Solar Electricity Transactive Markets

Jason Lin

Thesis submitted to the faculty of the Virginia Polytechnic Institute and State University
in partial fulfillment of the requirements for the degree of

Master of Science
In
Electrical Engineering

Saifur Rahman, Chair
Manisa Pipattanasomporn
Guoqiang Yu

December 11th, 2018
Arlington, Virginia

Keywords:
auction mechanism, blockchain, game theory, smart contract, transactive energy

jason.lin@vt.edu

Analysis of Blockchain-based Smart Contracts for Peer-to-Peer Solar Electricity Transactive Markets

Jason Lin

ABSTRACT

The emergence of blockchain technology and increasing penetration of distributed energy resources (DERs) have created a new opportunity for peer-to-peer (P2P) energy trading. However, challenges arise in such transactive markets to ensure individual rationality, incentive compatibility, budget balance, and economic efficiency during the trading process. This thesis creates an hour-ahead P2P energy trading network based on the Hyperledger Fabric blockchain and explores a comparative analysis of different auction mechanisms that form the basis of smart contracts. Considered auction mechanisms are discriminatory and uniform *k*-Double Auction with different *k* values. This thesis also investigates effects of four consumer and prosumer bidding strategies: random, preference factor, price-only game-theoretic approach, and supply-demand game-theoretic approach. A custom simulation framework that models the behavior of the transactive market is developed. Case studies of a 100-home microgrid at various photovoltaic (PV) penetration levels are presented using typical residential load and PV generation profiles in the metropolitan Washington, D.C. area. Results indicate that regardless of PV penetration levels and employed bidding strategies, discriminatory *k*-DA can outperform uniform *k*-DA. Despite so, discriminatory *k*-DA is more sensitive to market conditions than uniform *k*-DA. Additionally, results show that the price-only game-theoretic bidding strategy leads to near-ideal economic efficiencies regardless of auction mechanisms and PV penetration levels.

Analysis of Blockchain-based Smart Contracts for Peer-to-Peer Solar Electricity Transactive Markets

Jason Lin

GENERAL AUDIENCE ABSTRACT

The emergence of blockchain technology and increasing penetration of distributed energy resources such as solar panels have created a new opportunity for peer-to-peer (P2P) energy trading. As energy generation becomes more decentralized, utilities lose energy sales while local producers are undercompensated for reducing utility transmission losses and local buyers are overpaying for power. P2P energy trading creates a mutually beneficial relationship among all parties by offering buyers locally produced green energy, compensating local producers, and levying tariffs for use of existing utility infrastructures. In such transactive markets, communities enjoy cheaper electricity prices while supporting local green energy production. However, there exists considerable knowledge gap between market mechanisms and energy exchanges. Challenges arise in the trading process to ensure fairness for an unattainable ideal market. Thus, this thesis aims to offer insights for building the foundation of a P2P energy trading platform. An hour-ahead P2P energy trading network based on blockchain technology is created. A comparative analysis of different auction mechanisms is explored. Additionally, effects of four consumer and prosumer bidding strategies are investigated. A custom simulation framework that models the behavior of the transactive market is developed with case studies of a 100-home microgrid at various photovoltaic (PV) penetration levels presented. A key result indicates that the price-only game-theoretic bidding strategy leads to near-ideal economic efficiencies regardless of auction mechanisms and PV penetration levels.

ACKNOWLEDGEMENTS

First and foremost, I would like to thank my committee chair, Dr. Saifur Rahman, for giving me the opportunity to work under his guidance with his team. Dr. Rahman was willing to take a leap of faith and give me the chance of conducting research and writing a thesis in three short months – a process that normally takes at least a year to 1.5 years – when no other professors would. Dr. Rahman has opened new doors for me to the world of research and blockchain development. His continuous drive in academia and industry as the president of the IEEE Power and Energy Society is truly inspirational. Without Dr. Rahman's confidence in me, this thesis would not have been possible.

I would also like to express my deep gratitude for Dr. Manisa Pipattanasomporn, who was there for me every step of the way. Her endless patience, invaluable advice, and warm personality are a constant source of positive energy to which no problems can't be solved. Dr. Manisa truly wanted me to succeed and took a personal interest in my work. For example with exactly two weeks to the ISGT (Innovative Smart Grid Technologies) conference submission deadline, Dr. Manisa suggested that I make a submission – to which we produced my first ever paper to be published. In addition, Dr. Manisa took my dreams to heart and would regularly forward entrepreneurial opportunities to me. Without her unwavering support and guidance, this thesis would not have been possible.

I would like to extend my special thanks to Dr. Guoqiang Yu for providing his valuable time. Sincere gratitude to my supportive friends, Lavanya Murugesan, K Alnejar, Parker White, as well as my employer Mr. Michael Reardon, who urged me to finish my master's degree when I wanted to drop out of graduate school. Thank you!

TABLE OF CONTENTS

LIST OF TABLES

LIST OF FIGURES

LIST OF SYMBOLS AND ABBREVIATIONS

API	Application Programming Interface
DER	Distributed Energy Resource
k-DA	*k*-Double Auction
P2P	Peer-to-Peer
PBFT	Practical Byzantine Fault Tolerance
PoS	Proof of Stake
PoW	Proof of Work
PURPA	Public Utility Regulatory Policies Act
PV	Photovoltaic
REST	Representational State Transfer
TE	Transactive Energy
TR	Trade Reduction
VCG	Vickrey-Clark-Groves

B^P, S^P	Bid price and ask price, respectively
B_k^Q, S_j^Q	kWh quantity demanded/supplied by buyer *k* / seller *j*, respectively
N_B, N_S, N_T	Total number of buyers, sellers and trades, respectively
T_m^Q, T_m^P	Total kWh quantity transacted and transacted price for trade *m*, respectively
$\chi_i^{strategy}$	Potential bid/ask price of participant *i* when employing strategy *strategy* (low, same, high)
$U_i^{strategy}$	Utility of participant *i* when employing strategy *strategy* (low, same, high)
$\pi_i^{strategy}$	Payoff of participant *i* when employing strategy *strategy* (low, same, high)
$\delta_i^{strategy}$	Preference factor of participant *i* when employing strategy *strategy* (low, same, high)
ζ_i	Marginal cost of participant *i*
γ	Breakeven index

CHAPTER 1. INTRODUCTION

1.1 Background

To say that the U.S. power sector is undergoing a transformation has now become a cliché [1]. For its ~140 year existence, the U.S. electric grid is based on a centralized unidirectional system where power flows from large-scale generators to demand loads via transmission and distribution lines. However with the declining price of renewable energy technologies and the institution of green energy policies, the electric grid is transforming into a more decentralized system where power may be generated and consumed by prosumers. As of August 2018, there are more than 1.7 million prosumers supplying power back into the grid [2], representing only about 1.3% of total U.S. residential electric customers. Installation costs of photovoltaic (PV) systems has decreased ~28% from 2014 to 2018 [3], leading to more than a tripling of installed capacity from 3.3GW to 11GW in just four years [4].

It all started with the Public Utility Regulatory Policies Act (PURPA) of 1978, enacted in response to the 1973 energy crisis from an oil embargo from members of the Organization of Arab Petroleum Exporting Countries (OAPEC). In an effort to reduce demand, promote cogeneration as well as installation of renewable energy resources, the act required "power providers to purchase excess power from grid-connected small renewable energy systems at a rate equal to what it costs the power provider to produce the power itself" [5]. PURPA was amended by the Energy Policy Act of 1992 and further revised by the Energy Policy Act of 2005, which provided tax incentives and expanded renewable energy as well as distributed energy developments [6]. Specifically, the

Energy Policy Act of 2005 required states to consider adoption of net metering standards for energy generation as well as smart metering standards for time-based electric charges [7]. Depending on state regulations and each electric utility company, four main service models now exist for residential customers: fixed, tiered, time-of-use, and demand charge.

- Fixed rate – utility charges a set amount per kilowatt-hour used.
- Tiered rate – energy used over a set amount is billed at a different rate.
- Time-of-use rate – pricing differs based on peak/off-peak hours of the day; requires installation of special meter for time and energy reporting.
- Demand rate – billed based on averaged peak power demand during a set time interval, commonly 15-minute and 30-minute intervals. For example, using a 5kW dryer and 4kW range *at the same time* for the duration of the set period would incur a charge that is 9 times the demand charge rate. However, using them at different time periods would greatly reduce peak demand.

A sample electric bill is shown in Fig. 1. From this utility, Schedule 1 indicates a tiered rate where distribution and generation charges are lower once monthly consumption exceeds 800kWh [8]. A typical electric bill is composed of distribution service charges, electric supply service charges, sales & use surcharge, tax, as well as any applicable riders. Distribution service charges account for the use of overhead lines, underground cables, substations, and transformers used to deliver electricity from high-voltage transmission lines to end-use customers. Electric supply service charges cover generation (production of electricity), transmission (moving electricity from power plants

to substations), and fuel (costs associated with fuel used to produce electricity, including transportation). Lastly, riders are applied to certain rate schedules to recover the utility's cost of operation and electric production.

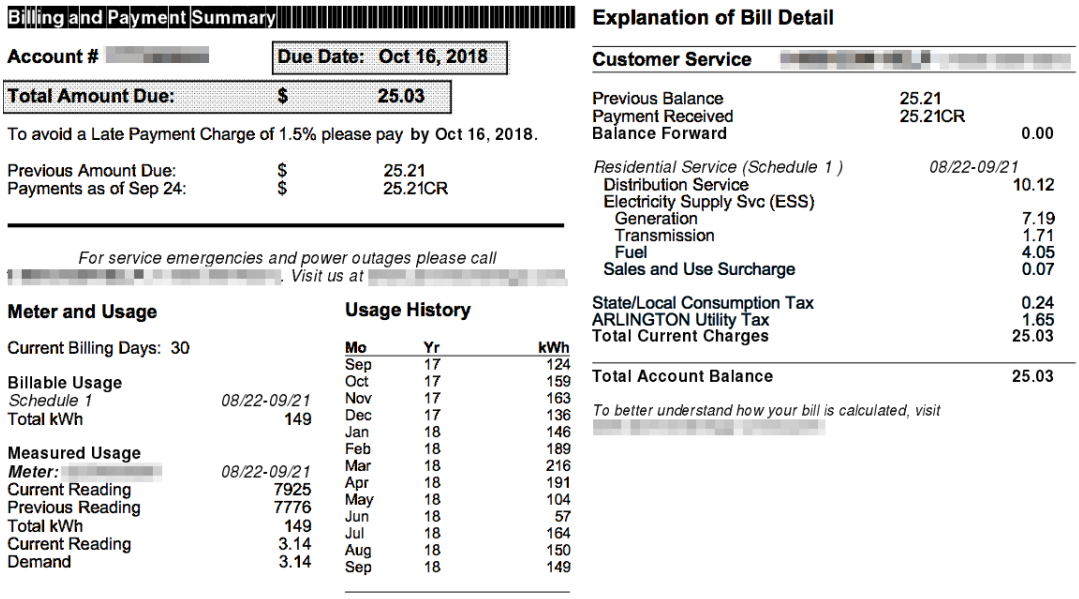

Billing and Payment Summary

Account # [redacted] **Due Date: Oct 16, 2018**

Total Amount Due: $ 25.03

To avoid a Late Payment Charge of 1.5% please pay by Oct 16, 2018.

Previous Amount Due:	$	25.21
Payments as of Sep 24:	$	25.21CR

For service emergencies and power outages please call [redacted]. *Visit us at* [redacted]

Meter and Usage

Current Billing Days: 30

Billable Usage	
Schedule 1	*08/22-09/21*
Total kWh	149
Measured Usage	
Meter: [redacted]	*08/22-09/21*
Current Reading	7925
Previous Reading	7776
Total kWh	149
Current Reading	3.14
Demand	3.14

Usage History

Mo	Yr	kWh
Sep	17	124
Oct	17	159
Nov	17	163
Dec	17	136
Jan	18	146
Feb	18	189
Mar	18	216
Apr	18	191
May	18	104
Jun	18	57
Jul	18	164
Aug	18	150
Sep	18	149

Explanation of Bill Detail

Customer Service [redacted]

Previous Balance	25.21	
Payment Received	25.21CR	
Balance Forward		0.00
Residential Service (Schedule 1)	*08/22-09/21*	
Distribution Service		10.12
Electricity Supply Svc (ESS)		
Generation		7.19
Transmission		1.71
Fuel		4.05
Sales and Use Surcharge		0.07
State/Local Consumption Tax		0.24
ARLINGTON Utility Tax		1.65
Total Current Charges		25.03
Total Account Balance		25.03

To better understand how your bill is calculated, visit [redacted]

Fig. 1. Sample electric bill.

While arrangements vary widely across localities, two main schedules currently exist to compensate prosumers for energy production:

- Net metering – requires one meter where customers are billed for their net energy use. Since the meter may run backwards, credits are at full retail rate [5]. Depending on each state, excess credits may or may not be rolled over to the following month.
- Feed-in tariff – requires two meters where energy production and consumption are measured and credited/billed separately. Depending on the jurisdiction, energy production may be sold at a premium rate or wholesale/avoided cost rate

to the utility company for the duration of a specified contract period, typically 15-20 years [5].

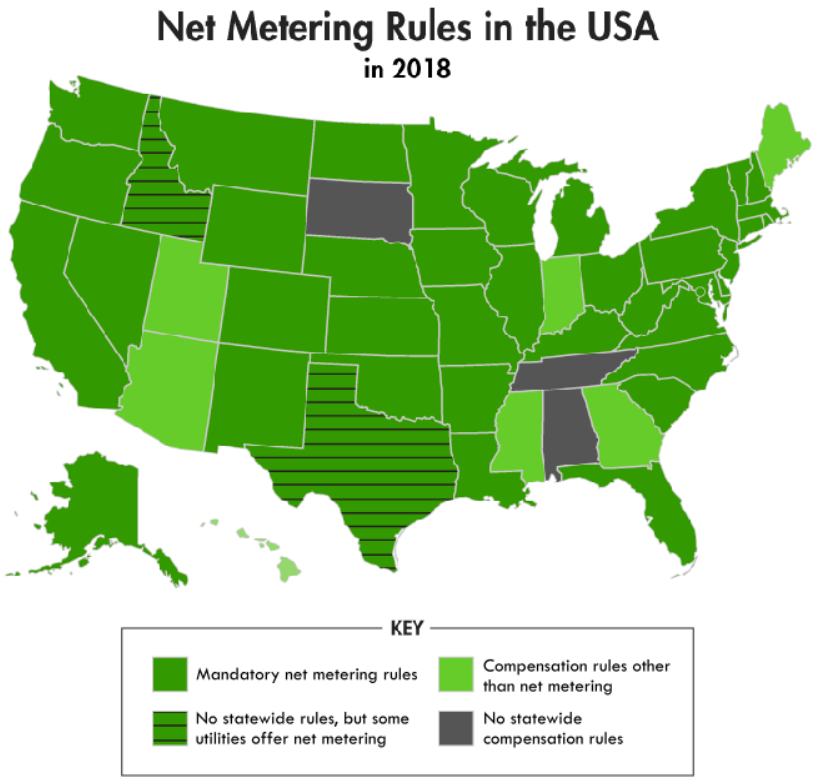

Fig. 2. 2018 Compensation rules for residential distributed energy generation.

As of October 2018, 38 states and Washington, D.C. have mandated net metering rules as exhibited in Fig. 2 [9]. While Idaho and Texas do not have statewide net metering regulations, some utilities have voluntarily adopted the program. Seven states (Arizona, Georgia, Hawaii, Indiana, Nevada, Maine, Mississippi) have alternate compensation plans such as feed-in tariffs. Certain feed-in tariff programs offer compensation at premium rates to encourage homeowners to install distributed energy resources (DERs). For example through the Experimental Advanced Renewable Energy Program, the state of Michigan offered residential customers a feed-in tariff of $0.24/kWh for a contract period of 15 years starting August 2009 and ending on August

2029 [10]. Such premium tariff is nearly double the average retail cost of electricity at $0.1268/kWh in August 2009 [11]. However, some states are beginning to phase out net metering rules and premium feed-in tariffs as penetration of DERs increase, opting for feed-in tariffs at or near the avoided cost rate. This significantly lower rate represents the marginal cost for a utility to produce one more unit of power. For example, Indiana's Senate Bill 309, which was enacted in May 2017, planned to phase out net metering by July 2022, starting December 2017 [12]. Afterwards, new DER owners will be compensated by at a rate of 1.25 times the utilities' avoided cost rate instead of the full retail rate. If such policy were enacted in August 2018, DER homeowners would be billed $0.1226/kWh for electric consumption while being compensated at only $0.0452/kWh for excess energy production [13], [14]. Rate design has been a hot debate especially for states with high PV penetration (Hawaii, California, Nevada, Arizona). Proponents of eliminating net metering argue that the policy unfairly transfers unrecovered operation and maintenance costs to the utilities and other non-DER owners [15]. While some studies supported this position, other cost-benefit analyses concluded that net metering benefits all parties [16], [17].

There is no doubt cost-benefit assessments may vary widely due to different markets, methodologies, as well as valuations. Despite so, one point is clear: as DER penetration increases, green energy policies that govern residential customers as well as businesses have to advance accordingly to establish win-win relationships. Consider two cases [18]:

- A single prosumer with a PV system and an electric vehicle that charges at home during the day.

- Two neighbors – one with a PV system and the other with an electric vehicle.

From a high-level power system perspective, the two scenarios are equivalent as local demand and supply are balanced. Thus, there is no impact on upstream power generation or transmission, resulting in the same costs to the utility. However, such is not the case from the residents' perspectives. In the first scenario, the prosumer may virtually charge their electric vehicle for free given excess generation from their PV system. In the second scenario, the electric vehicle owner will pay the retail rate of electricity as if it were supplied by a power plant many miles away. In actuality, the electricity used to charge the vehicle came from their neighbor. Thus, the electric vehicle owner was overcharged for transmission and its associated riders. The neighbor with the PV system may receive a feed-in tariff from the utility, perhaps near the avoided cost rate. In effect, the prosumer was undercompensated for providing a reduction in transmission losses as well as power congestion.

As the natural behavior of prosumers is to seek higher tariff rates and consumers lower electric charges, an opportunity is revealed: blockchain-enabled peer-to-peer (P2P) energy trading. In line with the grid's transformation into a more decentralized system, P2P energy trading may increase network resilience, provide monetary benefits for participants in a free market, allow individuals to exercise purchase decisions on alternative energy sources, and even foster a greater sense of community [19]. Blockchain technology further facilitates P2P energy trading by offering a higher level of trust, automation, and permanent record-keeping [20].

1.2 Objectives

As blockchain-based P2P energy trading emerges, there exists considerable knowledge gap between market mechanisms and energy exchanges. Thus, this thesis aims to offer insights for building the foundation of a P2P energy trading platform. The platform shall align interests of electricity consumers, prosumers, as well as power system operators within local communities. The research objectives are:

1. Implement a simple blockchain-based P2P energy trading network.
2. Design and analyze various blockchain-based smart contracts for solar electricity exchanges.

1.3 Contributions

In addition to briefly discussing potential market applicability of P2P energy trading within the U.S., major contributions of this thesis include the investigation of various auction mechanisms that form the basis of smart contracts to facilitate energy trading, evaluation of economic efficiencies of the smart contracts, and the implementation of a simple P2P energy trading platform based on the Hyperledger Fabric blockchain. In addition, a custom simulation framework that models the high-level behavior of the P2P energy trading blockchain network has been developed. Lastly, simulation case studies of a 100-home microgrid with varying degrees of PV penetration have been comparatively analyzed against four bidding strategies.

CHAPTER 2. LITERATURE REVIEW

This chapter provides a review of blockchain technology, an overview of current P2P energy trading implementations, and a survey of different auction mechanisms. Lastly, a summary of existing knowledge gaps is presented.

2.1 Blockchain Technology

2.1.1 Blockchain Architecture

Blockchain, fittingly, is a chain of digital blocks that contain transaction records like conventional ledgers. Blocks are sequentially chained to each other via hashes of the header of their respective parent blocks. Each block is composed of a block header and a block body. The block body contains a transaction counter as well as the transactions themselves. Typical block metadata consists of the following [21]:

- Block version: version number that defines the set of validation rules to follow
- Parent block header hash: a hash that links to the previous block
- Merkle root hash: a hash of all the transactions in the block
- Time: current timestamp in Unix epoch time
- nBits: the threshold for which a block's header hash must not exceed for the block to be valid
- Nonce: a random number that can only be used once as additional input to a hashing function; used to show proof of work

When a transaction is initiated on a blockchain, public key cryptography and digital signatures are used to identify and authorize accounts. A transaction is a data

package such as a traded monetary value or the result of executing a smart contract. The transaction is signed by its initiator via a private key and sent to a node that belongs to the blockchain network. The node then validates the data package with the user's public key and propagates it to other nodes, which additionally validates the package and propagates it to their peers until all nodes are reached. Meanwhile, valid transactions are aggregated into blocks. Through consensus mechanisms discussed in following section, the network reaches an agreement for the latest block to be chained to the blockchain [22].

2.1.2 Consensus Protocols

Consensus problems arise in distributed computing due to presence of faulty processes or deceptive nodes. The problem is modelled after the Byzantine Generals Problem, first described in 1982 [23]: a group of generals with their respective soldiers surround an enemy city. Each general has the option to attack or retreat. However, it is vital for all generals to agree on a single course of action – if even one retreats, the whole attack fails. To complicate matters, the generals are only able to communicate via messengers, who may fail to deliver messages correctly or completely. In addition, there may be traitorous generals. Similarly in blockchain, there is no guarantee that ledgers on various nodes (where data is stored) are all the same. Thus, a protocol to establish consensus is essential. Several consensus models are briefly reviewed below.

2.1.2.1 Practical Byzantine Fault Tolerance (PBFT)

PBFT is a practical model that improves the original BFT consensus through state machine replication [24]. Every node (replica) in the blockchain network maintains an

internal state and is ordered in sequence with one node being the primary node. Consensus is determined in four high-level phases:

1. Client sends a "service operation" request to the primary node.
2. Primary node multicasts the request to its secondary nodes.
3. All nodes process the request and send a reply to the client.
4. Client waits for f+1 replies with the same result and achieves consensus.

With n total number of nodes, BFT guarantees consensus given that there are no more than $f = \lfloor (n-1)/3 \rfloor$ faulty nodes.

2.1.2.2 Proof of Work (PoW)

Through proof of work [25], otherwise known as mining, nodes compute the cryptographic hash of the block's header. In the Bitcoin implementation, the resulting hash is required by consensus to be under a certain threshold, which is set by nBits in the block metadata. If the resulting hash is too large, the nonce, much like a salt, can be changed and the hash recomputed. This threshold changes dynamically every 2,016 blocks to ensure successful creation of one block every 10 minutes. Once a match is found, the miner is rewarded and the block cannot be changed without redoing the computational work. This is because any changes to the nonce or contents of the block also change the hash value. As blocks are chained after one another, any changes to a single block require re-computing the hashes for that specific block as well as all other blocks after it. If a mining pool is able to control 51% of the network's mining power, validation of new blocks can be suspended and transactions reversed or modified [26].

Another research indicates that this threshold can be decreased to only 25% via selfish mining [27].

2.1.2.3 Proof of Stake (PoS)

The proof of stake model was devised as an energy-saving alternative to PoW. Rather than consuming electricity to find a nonce, PoS requires validators to use their cryptocurrency as stake to purchase the ability to create blocks. While there are many PoS variants, Ethereum's implementation [28] requires new nodes to make significant security deposits set by its protocol. Linearly weighted by each node's security deposit, a validator is pseudo-randomly selected to create a block. If the block is successfully added to the chain, the validator receives a reward. If the validator acts in a malicious manner, they lose their security deposit and may no longer participate in the consensus process.

Table 1 provides a comparison of the reviewed consensus models [29].

Table 1. Comparison of consensus protocols.

	PBFT	**PoW**	**PoS**
Energy Saving	Yes	No	Partial
Dominance Threshold	≥25% computing power	≥51% stake	≥33.3% replicas
Example	Hyperledger Fabric	Bitcoin	Ethereum Casper

2.1.3 Blockchain Taxonomy

There are three main types of blockchain systems: public, private, and consortium. In public blockchains, all records are visible to the general public and anyone is permitted to join the consensus process. Since anyone can act as a node where records are stored, numerous copies exist in this decentralized network. Thus, transactions in a

public blockchain are considered immutable. Due to the large number of nodes in such network, propagation time is high and transaction throughput is limited.

On the other hand, private blockchains may restrict read access and only nodes from a single organization are allowed to join the consensus process. Since there are limited nodes and thus limited copies of blocks, records may be easily tampered. Due to the fewer number of nodes in this centralized network, propagation time is low and high transaction throughput may be achieved.

Consortium blockchains are a hybrid of public and private blockchains. Constructed by several organizations, the network allows pre-selected federated nodes to join the consensus process. Read access may be public or restricted as determined by the founding organizations. Due to the limited number of nodes, records are not completely immutable. Propagation time is low and transaction throughput is high in this partially centralized network.

Table 2 summarizes the three types of blockchain systems [21].

Table 2. Comparison of blockchain types.

	Public Blockchain	**Consortium Blockchain**	**Private Blockchain**
Read access	Public	Public or restricted	Public or restricted
Immutable	Yes	No	No
Efficiency	Low	High	High
Centralized	No	Partial	Yes
Consensus process	Permissionless	Permissioned	Permissioned

2.1.4 Comparison of Popular Blockchain Platforms

2.1.4.1 Ethereum

In an effort to improve on the limitations of Bitcoin, Ethereum [30] was proposed in 2013 by Vitalik Buterin at age 19 as an alternative blockchain for building decentralized applications. While the main Ethereum network is a permissionless public blockchain, it can be deployed as a permissioned private blockchain. In Ethereum, the order of transactions is crucial for maintaining a consistent state of the ledger. To reach consensus, Ethereum currently employs the PoW scheme while it is under transition to PoS [31]. Thus, the current PoW implementation unfavorably affects transaction processing time. Decentralized applications on Ethereum can make use of its built in cryptocurrency called Ether. Custom tokens may also be created via smart contracts.

2.1.4.2 Hyperledger Fabric

Hyperledger Fabric is part of an umbrella project hosted by The Linux Foundation with collaborative support from industry players. Launched in 2016 with focuses on modularity and business use across various industries, Hyperledger Fabric allows components such as consensus and membership services to be plug-and-play [32]. Thus, the platform may employ PBFT, PoW, PoS, or other consensus mechanisms based on the use case. In addition, Hyperledger Fabric is a private and permissioned blockchain that allows fine-grained access control of records. As such, privacy and performance are increased. In contrast to Ethereum, Hyperledger Fabric nodes assume different roles and tasks. These different nodes work together to reach consensus at the transaction level instead of the ledger level [33]. Because Hyperledger Fabric is intended for business use

across various industries, it does not have a built-in cryptocurrency. However, custom tokens can be created via smart contracts (chaincode).

Table 3 provides a comparison of the reviewed blockchain platforms [34].

Table 3. Comparison of popular blockchain platforms.

	Ethereum	**Hyperledger Fabric**
Description	Generic	Modular
Governance	Ethereum	The Linux Foundation
Type	Public/Private	Private
Consensus	PoW, ledger level	Pluggable, transaction level
Currency	Ether & custom tokens	Custom tokens

2.2 Overview of Current P2P Energy Trading Implementations

As of 2018, only a handful of P2P energy trading implementations exist in the world. The Brooklyn Microgrid is currently the only microgrid in the United States where residential neighbors have traded locally produced solar energy [35]. A trial was conducted in early 2016 with the system built on smart meters and the Ethereum blockchain [36]. During the three-month trial period, only two participants transacted in the market. The system has since shifted to a proprietary blockchain developed by the microgrid's operator company. Trading is done automatically by the platform and requires two user inputs – preferred energy sources and price limits. The market is uniformly cleared via a sealed-bid double auction in 15-minute intervals [37]. However, the trial was abandoned partially due to requiring regulatory approval – current U.S. regulations do not cover P2P energy trading [37].

Meanwhile, the Australian Renewable Energy Agency (ARENA) has awarded a $370,000 AUD feasibility project to be conducted on the Latrobe Valley Microgrid

starting March 2018 [38]. The project encompasses a local energy marketplace for dairy farmers, residents, as well as commercial/industrial customers in Latrobe Valley. In addition to trading solar energy, demand response capabilities will be incorporated as well. Other Australian projects include the Gen Y project at White Gum Valley. In this new community development, residents can share electricity harnessed from solar panels via P2P energy trading [39]. In Bangkok, the T77 precinct is currently conducting trials for energy trading between a shopping center, school, apartments, and a dental hospital [40]. According to a case study [41], the regulatory landscape of Thailand's energy sector can be very supportive of P2P energy trading; the Thai government has publicly identified benefits of such blockchain-enabled market. Projects in other parts of the world have been deployed as well. In the UK, the Piclo project hosts online auctions for demand response aggregators, energy suppliers, as well as vehicle charging operators [42]. The sonnenCommunity in Germany expands P2P energy trading with the use of batteries [43].

2.3 Auction Mechanisms

As the grid transforms with increasing DER integration, the conventional architecture of the utility network becomes less capable and more obsolete [44]. Thus, a transactive energy (TE) system that serves as a coordination mechanism is essential for efficient operation [45]. TE is defined as "a system of economic and control mechanisms that allows the dynamic balance of supply and demand across the entire electrical infrastructure using value as a key operational parameter" [46]. A novel approach to implementing such market is through P2P energy trading on blockchain technology. Thus, smart contracts form the foundation of the TE market in which auction mechanisms

are implemented. While the study of auction theory is beyond the scope of this thesis, the following sections briefly review several common mechanisms.

2.3.1 Discriminatory k-Double Auction (Discriminatory k-DA)

In *k*-DA [47], buyers submit sealed bid prices B^P while sellers submit sealed ask prices S^P for a single unit of a good. Following the natural ordering rule, bid prices are sorted in descending order while ask prices are sorted in ascending order. If $B^P \geq S^P$, a trade occurs at price p:

$$p = kB^P + (1 - k)S^P \qquad (1)$$

Where k is a predetermined constant in the (inclusive) closed interval $[0, 1]$. A k value in the (noninclusive) open interval $(0, 1)$ allows both buyers and sellers to influence the trading price. Thus, a k value of 0.5 sets the trading price at exactly between the bid price and the ask price. Neither party gains more utility than the other as in the case when k is either 1 or 0. When $k = 1$, trading price $p = B^P$. If $B^P > S^P$, the seller gains a utility of $B^P - S^P$ as the seller received more than the expected ask price. When $k = 0$, trading price $p = S^P$. If $B^P > S^P$, the buyer then gains a utility of $B^P - S^P$ as the buyer trades at a lower-than-anticipated price. This mechanism is discriminatory as the trading price is determined between each winning buyer-seller pair; no single market clearing price exists at each auction interval. Thus, trading prices differ between each winning buyer-seller pair.

2.3.2 Uniform k-Double Auction (Uniform k-DA)

The uniform *k*-DA mechanism is a variant of the discriminatory *k*-DA mechanism. In this mechanism, all winning participants trade at the same price. The market clearing price is determined by first sorting bids and asks according to the natural ordering rule, as in the case of discriminatory *k*-DA. Then, the largest breakeven index γ where $B_\gamma^P \geq S_\gamma^P$ is found. The market clearing price is then set as:

$$p = kB_\gamma^P + (1-k)S_\gamma^P \qquad (2)$$

where B_γ^P and S_γ^P are the bidding price and asking price at the largest breakeven index, respectively. Thus, the market clearing price is determined by the γ^{th} buyer and seller. This auction mechanism yields a single per-unit transaction price for all winning participants at each auction interval.

2.3.3 Vickrey-Clark-Groves (VCG)

In comparison to *k*-DA where participants may attempt to "game the system", the Vickrey-Clark-Groves (VCG) mechanism is motivates participants to bid truthfully at the expense of the market operator [48]. External subsidization is required to facilitate trades. To see this, winning buyers pay:

$$p_B = max(S_\gamma^P, B_{\gamma+1}^P) \qquad (3)$$

and sellers receive:

$$p_S = min(S_{\gamma+1}^P, B_\gamma^P) \qquad (4)$$

where $B_{\gamma+1}^P$ and $S_{\gamma+1}^P$ are the bid price and ask price following the largest breakeven index, respectively. Due to the natural ordering rule, $B_\gamma^P \geq B_{\gamma+1}^P$ as bids are sorted in descending order. Similarly, $S_\gamma^P \leq S_{\gamma+1}^P$ due to ask prices sorted in ascending order. Such forms the following solution matrix:

Table 4. VCG solution matrix.

	$\boldsymbol{S_{\gamma+1}^P > B_\gamma^P}$	$\boldsymbol{S_{\gamma+1}^P \leq B_\gamma^P}$
$\boldsymbol{S_\gamma^P > B_{\gamma+1}^P}$	$p_B = S_\gamma^P\,, p_S = B_\gamma^P$	$p_B = S_\gamma^P\,, p_S = S_{\gamma+1}^P$
$\boldsymbol{S_\gamma^P \leq B_{\gamma+1}^P}$	$p_B = B_{\gamma+1}^P\,, p_S = B_\gamma^P$	$p_B = B_{\gamma+1}^P\,, p_S = S_{\gamma+1}^P$

Since $p_B \leq p_S$, a deficit exists. Subsidization by the market operator is necessary to catalyze the trade. Thus, the minimum subsidy required to trade a single unit of good is $p_S - p_B$.

2.3.4 Trade Reduction (TR)

The Trade Reduction (TR) mechanism does not require external subsidization yet drives participants to bid truthfully. This occurs at the expense of the last winning buyer and seller: the TR method limits trades to $\gamma - 1$ buyers and $\gamma - 1$ sellers [48]. Such differs from uniform *k*-DA and VCG, where there areγwinning buyers and γ winning sellers. Because the γ^{th} buyer and γ^{th} seller are precluded from the TR auction, social welfare is not maximized. However, each trading buyer pays B_γ^P and each trading seller receives S_γ^P for a single unit of good. Since $B_\gamma^P \geq S_\gamma^P$, the market operator financially gains $B_\gamma^P - S_\gamma^P$ per unit of good from each transaction.

2.4 Mechanism Properties

This section briefly reviews four properties of an ideal auction mechanism: individual rationality, budget balance, incentive compatibility, and economic efficiency [47]. It is important to note that the Myerson-Satterthwaite theorem proves that these four conditions cannot exist simultaneously in any auction mechanism [49].

2.4.1 Individual Rationality

To satisfy individual rationality, no agent shall result in negative utilities from trading in the auction. Thus trading price $p \leq B^P$ and $p \geq S^P$, where B^P and S^P are the bid price and ask price, respectively. All four mechanisms discussed previously exhibit individual rationality as trades only occur when $B^P \geq S^P$.

2.4.2 Budget Balance

In order for a mechanism to be budget balanced, the market operator shall not financially subsidize or gain from the transactions between buyers and sellers. Thus, payments made by buyers must be equal to the amount received by sellers. Both discriminatory and uniform *k*-DA mechanisms are budget balanced as trade prices net zero between winning agents. The VCG method is not budget balanced as subsidy is necessary to facilitate trades. The TR approach is considered weakly budget balanced as the market operator is not required to subsidize trades but may financially gain from transactions.

2.4.3 Incentive Compatibility

Otherwise known as truthfulness and strategy-proofness, agents shall be motivated to bid their true valuations regardless of other players' strategies. Participants can thus ensure best outcomes when acting upon their true preferences. Both discriminatory and uniform *k*-DA are not incentive compatible as participants may submit offers different from their true valuations for individual gain. However, VCG ensures truthful bidding. Shown in equations (3) and (4), offers submitted by both buyers and sellers determine their abilities to transact as well as the transaction price. TR is also strategy-proof as winning participants have no incentive to bid otherwise. Non-participating γ^{th} buyer and γ^{th} seller may bid better than $B_{\gamma-1}^{P}$ or $S_{\gamma-1}^{P}$, respectively. However due to the natural ordering rule, the γ^{th} buyer will pay more than his original bid price and the γ^{th} seller will receive less than his original ask price. Such results in negative utilities, thus enforcing truthfulness.

2.4.4 Economic Efficiency

Economic efficiency, also known as social welfare, accounts for all individual utilities where a limited quantity of goods is allocated to those who value them the most. In *k*-DA and VCG, no participant is precluded from the trading in the market. Thus, both mechanisms are economically efficient. However, the TR method prohibits the γ^{th} buyer and γ^{th} seller from taking part in the auction. Therefore TR is not economically efficient.

2.5 Knowledge Gaps

As P2P energy trading is an emerging field, there exists a significant knowledge gap in the analysis of auction mechanisms for energy exchanges. The case for P2P energy trading was established in section 1.1, where two scenarios in which neighbors with/without a PV system/an electric vehicle were compared. Thus, the main goal of such transactive energy market is to fulfill alternative energy needs of both consumers and prosumers within the local community. While auction theory is commonly applied to areas such as communication networks and online advertising, its implementation in the context of P2P energy trading has not been investigated in detail. Different smart contracts can be formulated based on different auction mechanisms. However, economic efficiencies of various smart contracts have not been evaluated in current studies. In addition, performance of these auction mechanisms in response to different bidding strategies (e.g., game theory) has also not been explored in the context of a microgrid. Thus, these knowledge gaps serve as the basis of this thesis.

CHAPTER 3. METHODOLOGY

This section discusses the methodologies applied to implement a blockchain-enabled trading network as well as smart contracts and participant bidding strategies. Smart contracts are built on top of the energy trading network and define the market clearing process for submitted participant bids.

3.1 Blockchain-enabled Trading Network

3.1.1 Blockchain Platform Selection

Selection of the right blockchain platform for P2P energy trading has been an ongoing discussion, especially since many platforms and implementations are still in their demonstration phases. Regardless, certain key factors exist for the selection of a P2P energy trading blockchain platform. While not an exhaustive list, few desirable characteristics are:

- High privacy: Privacy is of concern as smart meters are able to monitor a home's electricity consumption as well as PV generation. This data is then passed onto the blockchain platform for processing of transactions. If energy trading occurs at real time instead of the proposed hour-ahead mechanism, load signatures of each home may be revealed on the ledger. Regardless, a private/consortium-based permissioned blockchain is key to maintaining privacy.

- Low transaction time: Confirmation of transactions should occur at or near real time. For example, confirmation of a block of transactions in Bitcoin is ~10 minutes [50]. The block time for Ethereum is ~12 seconds [51].
- Low energy use: As a platform applied to trading of excess solar energy, its energy consumption should be kept to a minimum.
- High scalability: High scalability allows expansion of business opportunities.

With these factors in mind, Hyperledger Fabric is selected as the platform of choice. It is a private and permissioned blockchain that operates on the efficient PBFT protocol instead of the energy-intensive PoW mechanism. In addition, it offers an extremely high throughput of 1,273 transactions per second, more than four times that of Ethereum's 284 transactions per second [52]. Lastly, Hyperledger Fabric's modularity allows high scalability to multi-organization energy trading networks.

3.1.2 Blockchain Platform Implementation

Implementation of Hyperledger Fabric v1.1 is conducted on a local virtual machine running Ubuntu 16.04 LTS. Hyperledger Composer v0.2 is used as a rapid development environment for fast prototyping of the P2P energy trading network. Prerequisite dependencies such as Docker Engine, Node, git, and Python 2.7 are installed. Then, two core components that form the business network are defined:

1. Model File (.cto) describes the resources – assets, participants, and transactions – used in the business network.
    - Assets are anything, physical or nonphysical, of value. Two assets are defined in this network: PV system, which is identified by an

assigned ID and linked to its homeowner; and kWhlisting, which is the auction listing containing all participant bids/asks. The kWhlisting asset is identified by a timestamped listing ID that specifies the time of auction opening as well as a state that defines whether the auction is accepting offers or closed.

- Participants are entities involved in the business network. In this implementation, homeowners are defined as the only type of participant. They are registered via a unique ID and available token balance, which is tied to the U.S. dollar.
- Transactions encompass any actions performed on assets. In this work, four transactions are defined: OpenListing, CloseListing, SubmitSell, and SubmitBuy. Note that each transaction requires the kWhlisting listing ID parameter to reference correct auction listing. The OpenListing transaction is initiated at the beginning of each hour to signal participants opening of auction. After receiving this broadcast signal, homeowners can initiate SubmitSell or SubmitBuy transactions where quantity of energy in kWh and offer price in $/kWh are submitted. CloseListing is initiated at the last minute of each hour to signal closing of auction and processing of submitted bids/asks.

2. Script File (.js) is functionally a smart contract that defines the transaction logic of the business network. In this work, the smart contract is executed when the CloseAuction transaction is initiated. When this occurs, submitted

bids/asks are sorted according to the natural ordering rule and the market is cleared using the discriminatory *k*-DA auction mechanism.

A summary of the model file is presented in Table 5. A timeline of the transaction process is illustrated below in Fig. 3.

Table 5. Summary of model file.

Assets	**Participants**	**Transactions**
PV └ PVID └ homeowner kWhlisting └ listingID └ state └ bids └ asks	homeowner └ agentID └ balance	OpenListing └ listingID CloseListing └ listingID SubmitSell └ listingID └ homeowner └ kWhsupply └ price SubmitBuy └ listingID └ homeowner └ kWhdemand └ price

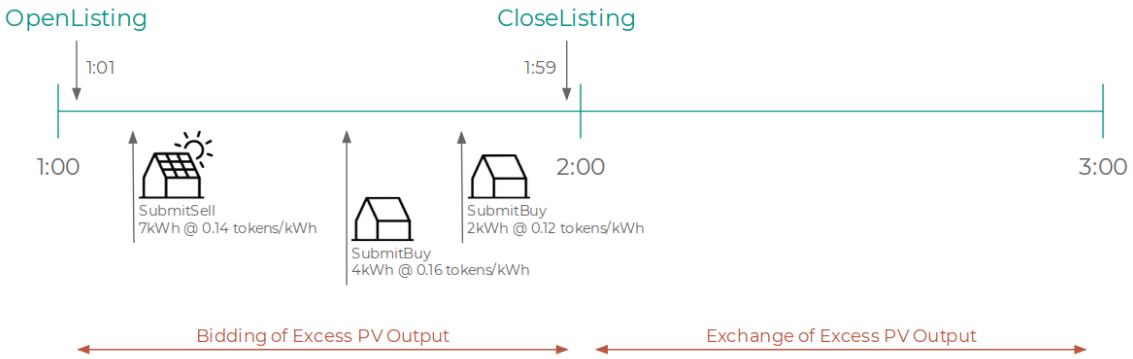

Fig. 3. Illustration of transaction timeline.

After these core files are defined, they are packaged into a business network archive. The archive is then deployed via Hyperledger Composer as a running business

network. A REST API (Representational State Transfer Application Programming Interface) is generated and REST server deployed to allow client applications to interact with the blockchain business network through HTTP requests (GET, PUT, POST, DELETE). In addition, an Angular 4 application running against the REST API is also generated by Hyperledger Composer. This gives developers a functional interface to explore the API.

To demonstrate basic P2P energy trading on Hyperledger Fabric, a single Python script that simulates six participants is created and executed on the same local virtual machine. The script interacts with the blockchain network via REST API with payload data in json format. First, the script registers the six homeowners with their respective unique agentIDs and initial balances. After successful registration, three homeowners register their PV assets with a unique random PVID along with their unique agentID. Then, the kWhlisting asset is created with the current timestamp as its listing ID and state set to OPEN. With the kWhlisting created, the OpenListing transaction is initiated – a broadcast message is sent to all participants, indicating start of bidding. The Python script listens for this broadcast message through a WebSocket connection. Once received, participants place offers to sell or buy excess PV energy for the next hour at randomized intervals. Then, the market is closed by initiating the CloseListing transaction with the associated listing ID. Now, the auction is closed and market is cleared through the specified auction mechanism in the smart contract. Balances as well as remaining kWh quantities for purchase/sale are updated. Conceptually in the last phase, both of these quantities are reconciled and updated on the blockchain through smart meters. However, this phase is not implemented due to being out of scope of this thesis.

3.2 Smart Contract

3.2.1 Auction Mechanism Selection

The selection and design of an appropriate auction mechanism for P2P energy trading are an art in itself and depend on usage contexts as well as operating legal environments. Despite being beyond the scope of this thesis, certain desirable characteristics exist for a mechanism to govern the auction process. For example, the mechanism should always be individually rational. The conditions for trading price $p \leq B^P$ and $p \geq S^P$, where B^P and S^P are the bid price and ask price, respectively, must always hold true. Otherwise, participants have no incentive to join the trading process as negative utilities may result. The mechanism should also be at least weakly budget balanced. This ensures that no external subsidy is required to catalyze trades. Other desirable characteristics include incentive compatibility and economic efficiency. However as mentioned previously, no auction mechanism can satisfy all four characteristics. For the purpose of this thesis, discriminatory and uniform *k*-DA are selected as the mechanisms of interest as they are the most commonly used auction processes. Both discriminatory and uniform *k*-DA exhibit individual rationality, budget balance, and economic efficiency.

3.2.2 Economic Efficiency Evaluation Metrics

Performance of auction mechanisms should be evaluated to maximize benefits for all participants. Mechanism properties such as individual rationality, budget balance, and incentive compatibility are predetermined by the formulation of mechanism itself. However, a mechanism's degree of economic efficiency has to be quantitatively analyzed

[53]. This thesis quantifies economic efficiency from the perspectives of the sellers, buyers, and microgrid operator. The three metrics, defined below, are: percentage of kWh sold, percentage of kWh bought, and percentage of households cleared. These performance metrics are calculated at each hourly auction interval and averaged for the duration of availability of excess solar energy generation.

3.2.2.1 Percentage of kWh Sold

The percentage of kWh sold assesses consumption of total supply from the sellers' perspective. It is defined as the ratio of the total kWh traded to the total kWh supplied for sales, formulated in (5). The higher the ratio, the higher sellers' excess PV outputs are successfully traded.

$$\sum_{m=1}^{N_T} T_m^Q \Big/ \sum_{j=1}^{N_S} S_j^Q \qquad (5)$$

3.2.2.2 Percentage of kWh Bought

The percentage of kWh bought evaluates fulfillment of total demand from the buyers' perspective. It is defined as the ratio of the total kWh traded to the total kWh demanded for purchase, as in (6). The higher the ratio, the higher buyers' demands are met.

$$\sum_{m=1}^{N_T} T_m^Q \Big/ \sum_{k=1}^{N_B} B_k^Q \qquad (6)$$

3.2.2.3 Percentage of Households Cleared

The percentage of households cleared quantifies fulfillment of the amount of buyer and seller contracts submitted at each hourly auction interval. It is defined as the ratio of total participants whose orders have been completely filled to the total number of participants in the microgrid, as in (7). Note the use of Iversion brackets, where the expression evaluates to 1 if true; 0 otherwise. Because demanded and supplied quantities may differ for each participant, B_k^Q and S_j^Q are updated upon each successful transaction to reflect the quantities remaining to be purchased and sold, respectively. The higher the ratio of households cleared, the higher the number of participants satisfied within the microgrid.

$$\frac{\sum_{k=1}^{N_B}[B_k^Q = 0] + \sum_{j=1}^{N_S}[S_j^Q = 0]}{N_B + N_S} \qquad (7)$$

Where,

N_B, N_S, N_T	:	Total number of buyers, sellers and trades
B_k^Q	:	kWh quantity demanded by buyer *k*
S_j^Q	:	kWh quantity supplied by seller *j*
T_m^Q	:	Total kWh quantity transacted for trade *m*

3.3 Agent Bidding Strategies

In this study, offers from each buyer/seller consist of bid/ask prices as well as the kWh quantity to be purchased/sold, respectively. kWh quantities to be purchased and sold

are based on the load/PV forecasts for the next hourly interval as discussed in section 4.1. Agent behaviors are modeled according to the following four bidding strategies:

3.3.1 Random Bidding Strategy

Bid/ask prices are randomly generated according to a uniform distribution between \$0.01/kWh and \$1/kWh, inclusive. This assumes random consumer and prosumer behavior and disregards the average retail cost of electricity.

3.3.2 Preference Factor Bidding Strategy

Bid/ask prices are generated from a preference factor of the previous-hour market price. The discount/markup factor resembles a household's preference to bid/ask more or less than the previous-hour market rate. This takes into account social factors where certain consumers may be willing to pay more for locally produced green energy. Certain prosumers may also be willing to sell at a lower price for the benefit of the community. Such behavior is modeled via sampling a normal distribution with a mean of 0.2 and standard deviation of 0.15. This assumes that most buyers seek a 20% discount from market rates and that most sellers seek a 20% premium from market rates. Since discriminatory auction mechanisms do not have a uniform market clearing price at each auction interval, the historical market price is determined by the weighted average of all transactions during the auction interval:

$$P_{seed} = \frac{\sum_{m=1}^{N_T} T_m^Q * T_m^P}{\sum_{m=1}^{N_T} T_m^Q} \qquad (8)$$

Since P_{seed} is not available for the first hour of the very first trade, it is set as the average of $P_{wholesale}$, the wholesale/avoided cost rate of electricity, and P_{retail}, the average retail cost of electricity, in a specified location.

3.3.3 Game-Theoretic Bidding Strategies

Bid/ask prices are generated from a game-theoretic approach. The formulated game is modeled as non-cooperative, simultaneous-move, and non-zero-sum. In non-cooperative games, all agents act strategically to maximize self-interests. Due to the large number of participants, cooperative games employing trigger strategies are not appropriate. The game is also modeled as simultaneous as all agents submit sealed bids without knowledge of the actions of other players. To simplify the game, buyers bid against all other buyers while sellers bid against all other sellers. Each participant has three strategies: to bid lower, same, or higher than the market price from the previous hour. The degree of bidding deviation from the previous-hour market rate is determined by each agent's low and high preferences. Similar to the second bidding strategy, these two preference factors ($\delta_i^{strategy}$) are generated via sampling a normal distribution with a mean of 0 and standard deviation of 0.15. The low preference factor is constrained to a negative value while the high preference factor is constrained to a positive value. Participant *i* can thus place a potential bid/ask price ($\chi_i^{strategy}$) of:

$$\chi_i^{strategy} = P_{seed} * (1 + \delta_i^{strategy}) \qquad (9)$$

where P_{seed} is the seed price (\$/kWh) from the previous-hour market rate and $\delta_i^{strategy}$ is the preference factor for each of the three strategies. In turn, the utility in \$/kWh for

participant i can be defined as $U_i^{strategy} = \zeta_i - \chi_i^{strategy}$ for buyers and $U_i^{strategy} = \chi_i^{strategy} - \zeta_i$ for sellers, where ζ_i is the marginal cost (\$/kWh) of participant *i*, given below:

$$\zeta_i = \begin{cases} P_{retail} & , \text{ participant } i \text{ is a buyer} \\ \frac{P_{install}}{\tau * \lambda} & , \text{ participant } i \text{ is a seller} \end{cases} \quad (10)$$

The buyer's "marginal cost" is assumed to be the average retail cost of electricity from the utility company. This represents the cost to acquire an additional kWh (\$/kWh) from the electric utility. The buyer may thus gain a high utility when there exists a high differential between the cost of electricity from the utility company and the P2P energy trading network.

On the other hand, the seller's marginal cost is the cost to generate an additional kWh of electricity (\$/kWh) over the useful life of their installed PV system. This is defined as the ratio of total installed PV system cost (\$), including operation and maintenance costs, to the annual forecast of generation (kWh) multiplied by its useful life, typically 20 years. This simplified model does not take into account degradation of PV panels over time. In this study, total installed PV system cost for each prosumer is calculated by:

$$P_{install} = P_{est} * 1000 * A_{roof} * 0.7 * 6.44/485 \quad (11)$$

Where P_{est} is the system cost per watt (\$/W), including annualized operation and maintenance costs, randomly generated from the closed interval [3.00, 4.50] [54] and A_{roof} is the one-sided area of the gable roof in square feet. With all necessary

information defined and utilities calculated, the normal-form game can be constructed as follows:

Table 6. Normal-form game.

		All Other Buyers/Sellers		
		χ_{others}^{lower}	χ_{others}^{same}	χ_{others}^{higher}
Participant i	χ_i^{lower}	$\pi_i^{lower}, \pi_{others}^{lower}$	$\pi_i^{lower}, \pi_{others}^{same}$	$\pi_i^{lower}, \pi_{others}^{higher}$
	χ_i^{same}	$\pi_i^{same}, \pi_{others}^{lower}$	$\pi_i^{same}, \pi_{others}^{same}$	$\pi_i^{same}, \pi_{others}^{higher}$
	χ_i^{higher}	$\pi_i^{higher}, \pi_{others}^{lower}$	$\pi_i^{higher}, \pi_{others}^{same}$	$\pi_i^{higher}, \pi_{others}^{higher}$

Where $\pi_i^{strategy}$ represents the payoff of participant *i* when the corresponding strategy is chosen. This thesis presents two payoff determination methods: price-only approach and supply-demand approach.

3.3.3.1 Price-Only Approach

In the price-only approach, participants compete to bid for the best price and are not knowledgeable of market supply and demand for excess PV energy. Thus, their payoffs can be determined by:

$$\pi_i^{strategy} = \begin{cases} U_i^{strategy}, & \chi_i^{strategy} < \chi_{others}^{strategy} \\ 0, & \text{otherwise} \end{cases} \quad (12)$$

$$\pi_{others}^{strategy} = \begin{cases} U_{others}^{strategy}, & \chi_{others}^{strategy} \leq \chi_i^{strategy} \\ 0, & \text{otherwise} \end{cases} \quad (13)$$

when participant *i* is a seller. Due to the natural ordering rule, sellers must bid lower than all other sellers in order to win a non-zero payoff. In contrast, the collective of "all other sellers" may bid equal to participant *i* to win a non-zero payoff. Because the collective has a greater number of sellers, it is assumed that they have a higher possibility of winning the bid than the individual seller. When participant *i* is a buyer, their payoff can be determined by

$$\pi_i^{strategy} = \begin{cases} U_i^{strategy}, & \chi_i^{strategy} > \chi_{others}^{strategy} \\ 0, & \text{otherwise} \end{cases} \quad (14)$$

$$\pi_{others}^{strategy} = \begin{cases} U_{others}^{strategy}, & \chi_{others}^{strategy} \geq \chi_i^{strategy} \\ 0, & \text{otherwise} \end{cases} \quad (15)$$

In the same way, individual buyers must bid higher than all other buyers in order to win a non-zero payoff; the collective of "all other buyers" must bid at least higher than participant *i* to win a non-zero payoff. Such describes a "winner-takes-all" situation.

This payoff determination method only takes into account pricing of electricity and assumes that participants have no knowledge of total quantities supplied and demanded in the market. Sellers always attempt to offer the lowest prices while buyers always attempt to bid the highest prices regardless of market condition.

3.3.3.2 Supply-Demand Approach

If agents are knowledgeable of excess PV supply and demand within the market, such information may be used to formulate different payoff matrices for buyers and sellers. For example when $demand > supply$ is projected for the next hourly interval, a

sellers' market results. Competition among buyers to place winning bids is high. Thus, buyers employ the above price-only payoff logic in an effort to bid the highest price. However, prosumers need not compete as intensely with other prosumers due to limited supply. Thus, the payoff determination logic for sellers is:

$$\pi_i^{strategy} = U_i^{strategy} \quad (16)$$

$$\pi_{others}^{strategy} = U_{others}^{strategy} \quad (17)$$

In this situation, both the individual seller and the collective of "all other sellers" have non-zero payoffs without any imposed conditions. Such win-win situation presumes that the limited supply of excess PV energy will be totally consumed by buyers. Thus, sellers may maintain their prices without loss when competing against all other sellers.

3.3.3.3 Finding Nash Equilibrium (NE)

Dominant strategies for each player can be identified if they result in the highest payoffs regardless of the opponent's strategy. Thus a Nash Equilibrium (NE) can be identified when, given the strategies of other players, no player can improve his payoff by changing his own strategy. Table 7 shows an example of a generated game for a consumer employing the price-only approach during simulation.

Table 7. Sample game during simulation.

		All Other Buyers		
		Lower	Same	Higher
Participant i	Lower	0.0578 , 0	0 , 0.0452	0 , 0.0338
	Same	0.0452 , 0	0 , 0.0452	0 , 0.0338
	Higher	0.0192 , 0	0.0192 , 0	0.0192 , 0

In this case, two Nash Equilibria are identified in terms of (row, column): (3,2) and (3,3). Participant i randomly selects one of these two NE and bids $P_{seed} * (1 + \delta_i^{strategy})$. For simplicity, no other strategies for choosing the best NE are employed.

Since a simple and easy-to-use NE solver is not readily available, the author coded his own. First, the two-player game is set up through a three-dimensional matrix of size $m \times m \times 3$, where m is the number of available strategies for each player. When $m = 3$, the game resembles that of Table 6 with the third element of each cell indicating the cell index (called 'strategy index' or 'si' in the pseudo code below):

$$game = \begin{bmatrix} [\pi_i^{lower}, \pi_{others}^{lower}, 1] & [\pi_i^{lower}, \pi_{others}^{same}, 2] & [\pi_i^{lower}, \pi_{others}^{higher}, 3] \\ [\pi_i^{same}, \pi_{others}^{lower}, 4] & [\pi_i^{same}, \pi_{others}^{same}, 5] & [\pi_i^{same}, \pi_{others}^{higher}, 6] \\ [\pi_i^{higher}, \pi_{others}^{lower}, 7] & [\pi_i^{higher}, \pi_{others}^{same}, 8] & [\pi_i^{higher}, \pi_{others}^{higher}, 9] \end{bmatrix}$$

This three-dimensional array is created with the format *game*[row][column][player payoff or strategy index]. The pseudo code for finding the NE is provided below. Note that this is by no means the most efficient method for finding the solution.

Nash Equilibrium finder pseudo code

```
//for each player
for p=0 : 2
       //test the player's strategy given other's move
       for k=0 : m
              for j=0 : m
                     //store player's utility in temp[j]
                     temp[j] = game[!p?j:k][!p?k:j][p]
              end for

              n = index/indices of max value(s) in temp[j]
              calculate 'si' by (!p?k:n)+1+m*(!p?n:k)
              concatenate solution to NE
         end for
end for

discard non-duplicate strategy indices in NE
randomly pick an element from available solutions in NE
if NE is empty
         randomly select a strategy in game
end if
```

CHAPTER 4. CASE STUDIES & RESULTS

This section discusses the context of conducted case studies in terms of geographical region, house characteristics, and load and PV generation profiles. Also discussed are the various simulated scenarios with their respective results presented.

4.1 Context

A hypothetical microgrid of 100 homes in the Washington, D.C. metropolitan area is targeted. The average retail cost of electricity is $0.1234/kWh and the average wholesale rate of electricity is $0.033/kWh [13]. In this region, typical single family homes are either single-story or two-stories tall, ranging from 1,000 to 4,000 square feet. To simulate such microgrid, a uniform distribution of house sizes is randomly generated within the aforementioned criteria. Load profiles and PV production profiles are generated as described below.

4.1.1 Load Profile

The hourly load profile used in this study is based on the Building America Housing Simulation B10 Benchmark obtained from the U.S. Department of Energy [55]. The obtained data represents an average load profile for a typical home in the Washington, D.C. metropolitan area. Only load data for a 24-hour period during the hottest summer month of August is used [56]. Fig. 4 illustrates the typical load profile for an average house size of 2,546 square feet. This base load profile is scaled proportionally to the previously generated home size. Additionally, a random ±20% deviation is introduced to induce variability.

4.1.2 PV Generation Profile

The hourly PV generation profile is obtained from a 6.44kW PV installation at a Virginia Tech building in Arlington, Virginia [57]. Shown in Fig. 4, the base PV generation profile represents a sunny summer day based on the installed PV system with a total panel area of 485 square feet.

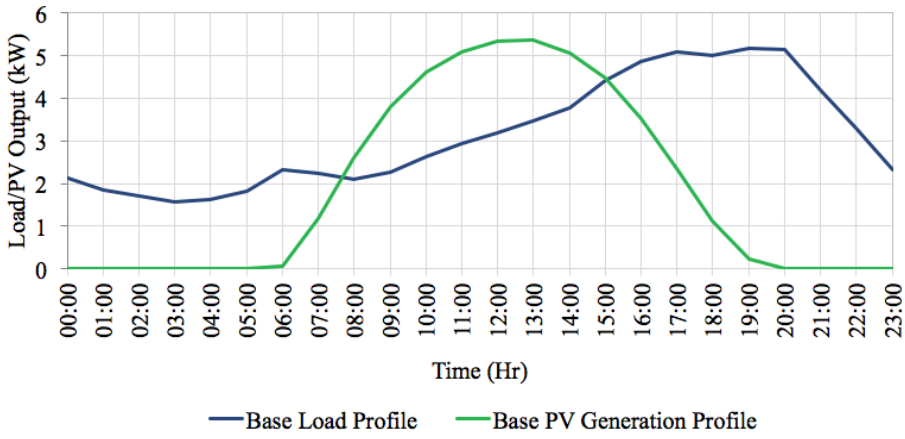

Fig. 4. A 24-hour load/PV generation profile.

The PV generation profile for each prosumer is determined by scaling the base PV profile to the size of usable roof space of each home. With each home ranging from 1,000 to 4,000 square feet, foundation area is assumed to range from 1,000 to 2,000 square feet. All homes are assumed to have gable roofs (Fig. 5) as they are considered to be one of the most suitable roof types for PV installation [58]. Conventional roof pitches (slopes) for residential homes range from the closed interval $\tan\theta = [4/12, 9/12]$ [59]. Through reverse area projection, single-side roof space (A_{roof}) can be derived from the area of foundation ($A_{foundation}$) as follows:

$$\cos\theta = \frac{0.5 * A_{foundation}}{A_{roof}}$$

$$\text{Thus, } A_{roof} = 0.5 A_{foundation} \cos^{-1}\theta \qquad (18)$$

Additionally, approximately only 70% of roof space can be utilized for PV installation [60]. A random ±20% deviation is also introduced to the hourly PV generation profile to account for variations in efficiency, tree shading, cloud coverage, etc.

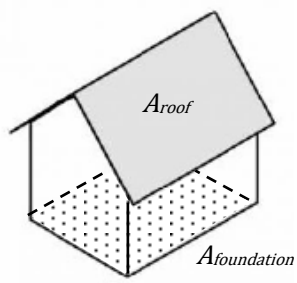

Fig. 5. Gable roof.

4.2 Simulated Scenarios

Fig. 6 proposes the various scenarios that are studied over a 24-hour period. For a microgrid of 100 homes, three PV penetration levels are tested (30%, 50%, 70%) with four participant bidding strategies (random, preference factor, price-only game theory, and supply-demand game theory). Offer prices from all participants are sorted according to the natural ordering rule. Both discriminatory and uniform *k*-DA mechanisms are tested with three degrees of *k* values: 0, 0.5, and 1. While a Hyperledger Fabric blockchain network is created with an interacting Python script, this configuration presents limitations in terms of scalability and execution time. Due to the number of operations for each participant during each hour for each auction mechanism and each PV penetration level, memory usage, transaction speed, as well as network communication speed over the REST API and WebSocket connection are of great

concern. Thus, the author has developed a custom simulation framework from the ground up that models the high-level behavior of the P2P energy trading blockchain network. The framework allows any number of defined auction mechanisms, ordering rules, bidding strategies, microgrid sizes, and buyer/seller ratios to be plugged into the simulation. In addition, the simulation framework supports arbitrary duration datasets.

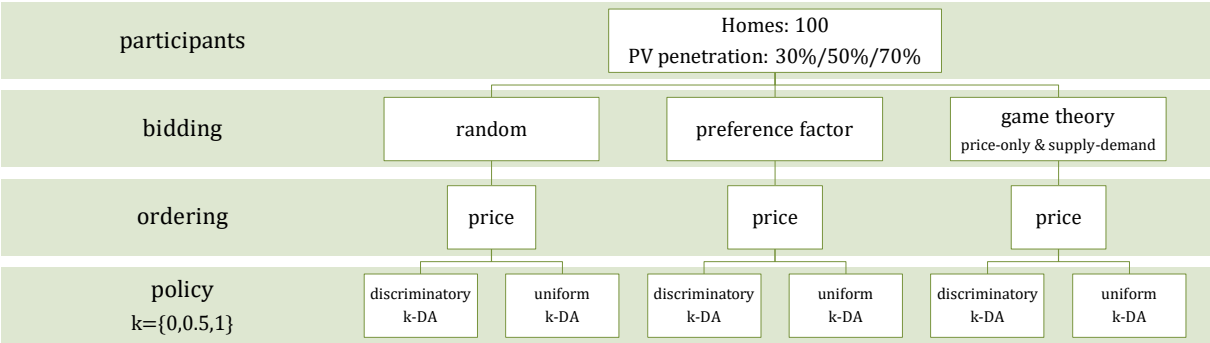

Fig. 6. Simulated scenarios.

4.3 Results & Discussions

4.3.1 Case I: 30% PV Penetration

Fig. 7 represents the 24-hour load and PV output profiles for a microgrid of 70 consumers and 30 prosumers. Note that the load profile for the 70 consumers is stacked on top of the aggregate load profile for the 30 prosumers. The summation of these two profiles indicate total load of the microgrid. Due to a 30% prosumer to consumer ratio, total prosumer load is lower than the total consumer load. As shown, the peak load of this microgrid is ~500kW between the hours of 17:00 and 20:00.

At 30% PV penetration, the total PV capacity in this microgrid is 263.9kW; peak PV output is ~200kW from 11:00 to 14:00. There is excess solar energy production from

the prosumers between ~07:30 to 16:00 that can be traded among neighbors within the microgrid.

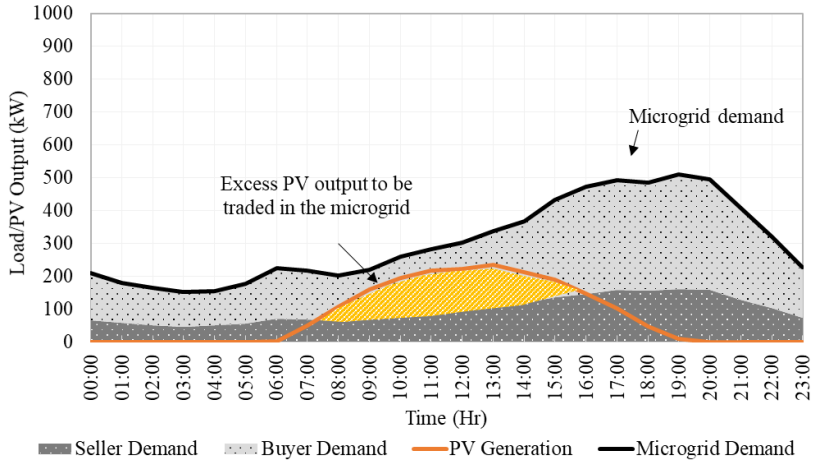

Fig. 7. Microgrid supply vs demand at 30% PV penetration.

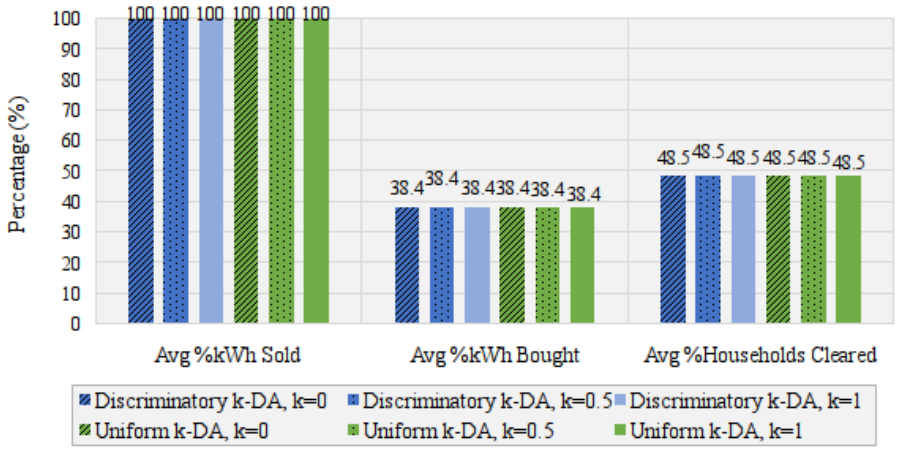

Fig. 8. Ideal market performance at 30% PV penetration.

If all participants bid exactly the same price, the ideal market performance shown in Fig. 8 would result regardless of auction mechanisms or bidding strategies. Such is valid as only quantities supplied and demanded are taken into account. Thus, the average percentage of kWh sold is 100% because all excess generated PV energy (yellow shaded area in Fig. 7) can be consumed by buyer demand. Similarly, the average percentage of kWh bought is 38.4% as this is the ratio between excess PV output (yellow shaded area)

and buyer demand (light-gray shaded area) for the duration of excess PV generation. At 30% PV penetration, this ideal scenario can completely fulfill orders of, on average, 48.5% of all households in the microgrid.

4.3.1.1 Random Bidding Strategy

When bidding prices are determined at random, results in Fig. 9 indicate that discriminatory *k*-DA offers the same average percentage of kWh sold/bought and households cleared as those of uniform *k*-DA. This indicates that discriminatory *k*-DA is able to fulfill the same amount of orders in the market as uniform *k*-DA when bid/ask prices/quantities are unchanged throughout the variation of *k* values. Varying degrees of *k* values do not affect trading outcomes for discriminatory *k*-DA nor for uniform *k*-DA. This makes sense as the condition $B^P \geq S^P$ must occur in both discriminatory and uniform *k*-DA for respective participants to trade; the *k* value only affects the trading price between winning buyers and sellers, indicated in equation (1) and equation (2). Thus, both auction mechanisms result in the same number of trading participants and economic efficiencies.

Fig. 9. Performance comparison for random bidding strategy at 30% PV penetration.

4.3.1.2 Preference Factor Bidding Strategy

Results of participants employing the preference factor bidding strategy are shown in Fig. 10. As expected, the average percentage of households cleared, which indicates the average percentage of fulfilled market orders, is extremely low. This is expected as most sellers submit bids higher than the market rate while most buyers submit bids lower than the market rate. Recall the *k*-DA mechanism and the property of individual rationality, the conditions $p \leq B^P$ and $p \geq S^P$ must exist for a trade to occur. Thus, the non-zero result in Fig. 10 is contributed by buyers or sellers whose preference factors are less than 0. These buyers and sellers do not seek discounts and premiums from market rates, respectively. Instead, these buyers are willing to pay more for locally generated green energy and these sellers are willing to gain less from market rates. These participants represent households whose preferences are to support the local community as well as green energy production.

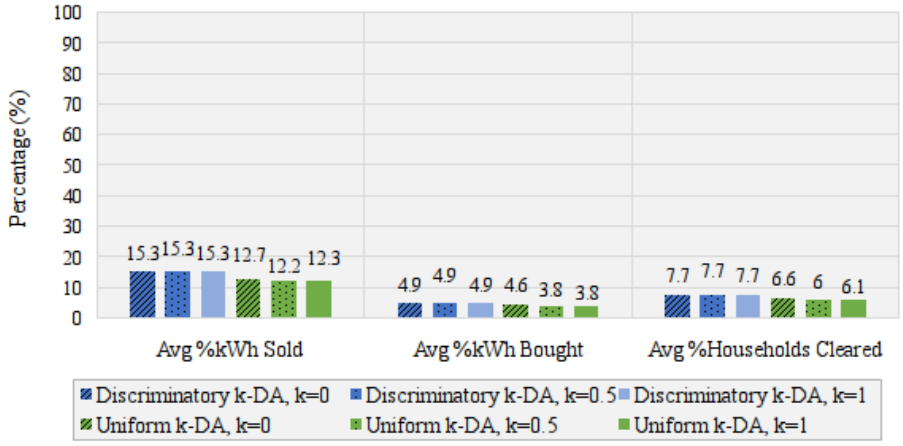

Fig. 10. Performance comparison for preference factor bidding strategy at 30% PV penetration.

4.3.1.3 Price-Only Game-Theoretic Bidding Strategy

Results in Fig. 11 compare the two *k*-DA auction mechanisms when participants bid using game theory with price-only payoff logic. In contrast to scenario 4.3.1.1 (random bidding strategy, 30% PV penetration) where the performance of discriminatory *k*-DA is maintained regardless of *k* value, performance under the game-theoretic approach changes with varying *k* values. Such is expected as the implementation depends on previous-hour market rates while the random bidding strategy does not. A simulation log of resulting hourly market rates is shown in Table 9 in the Appendix section.

Bidding with the price-only game-theoretic strategy is nearly ideal in a microgrid with 30% PV penetration. The implementation attempts to optimize each participant's bid price among their peers: buyers attempt to bid the highest price over all other buyers; sellers attempt to bid the lowest price over all other sellers. Because market supply and demand are not taken into account in the bid price determination process, this results in high economic efficiency as all participants try to offer accommodating prices.

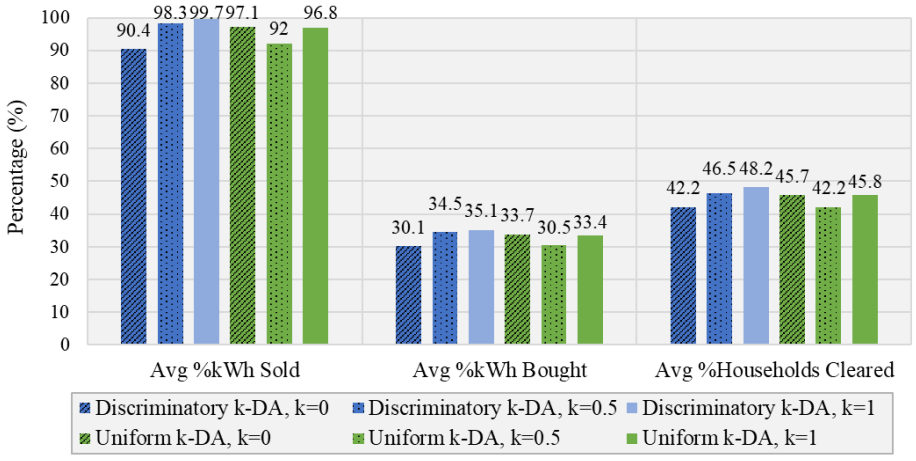

Fig. 11. Performance comparison for price-only game theory strategy at 30% PV penetration.

4.3.1.4 Supply-Demand Game-Theoretic Bidding Strategy

Despite results of scenario 4.3.1.3 (price-only game-theoretic approach, 30% PV penetration) being near-ideal, results of bidding with the supply-demand payoff logic as shown in Fig. 12 are far from ideal. Such can be attributed to the high asking prices from the prosumers as there is greater demand than supply, indicated in Fig. 7. This leads to high market rates and low transaction volumes. Such is evident in Table 10, where hourly trading prices are higher than those of the price-only method in Table 9. Also evident is the increase of market rates as *k* increases. In turn, fewer participants are able to "clear" market rates. As such, market price for certain mid-day auction periods are null – due to no transaction volume. This explains why there is a downward trend in performance as *k* increases.

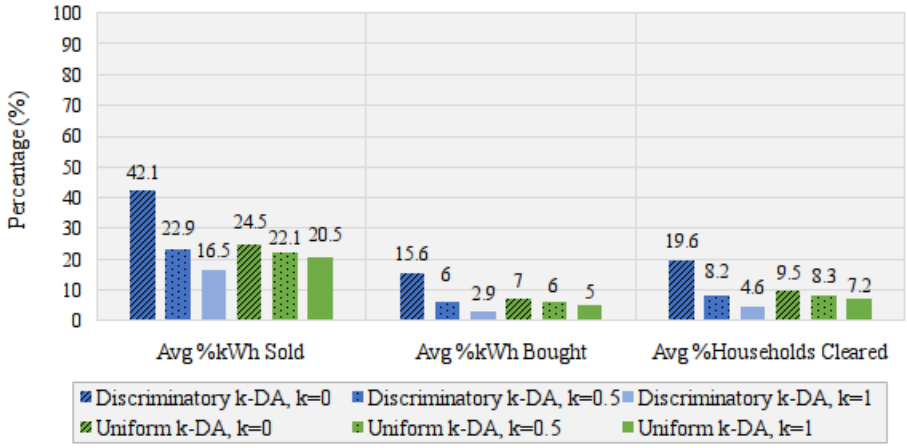

Fig. 12. Performance comparison for supply-demand game theory strategy at 30% PV penetration.

4.3.2 Case II: 50% PV Penetration

Fig. 13 shows the load and PV generation profiles for the microgrid at 50% PV penetration. The total prosumer load approximately mirrors the total consumer load due to the 50/50 seller/buyer ratio. The total PV capacity in this scenario is 456.4kW; peak

PV output is around 390kW at around 13:00. Similar to Case I, excess solar power is available for trade from ~07:30 to 16:00. Due to a higher PV penetration, there is an excess of PV output between ~08:30 to ~13:30 from the microgrid even after satisfying the microgrid's demand. The total microgrid demand profile is exactly identical to that of Case I, ensuring fair comparison between tested scenarios.

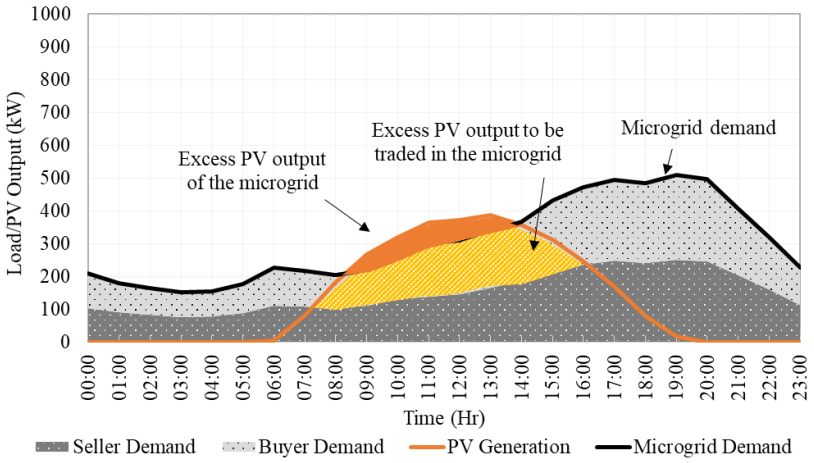

Fig. 13. Microgrid supply vs demand at 50% PV penetration.

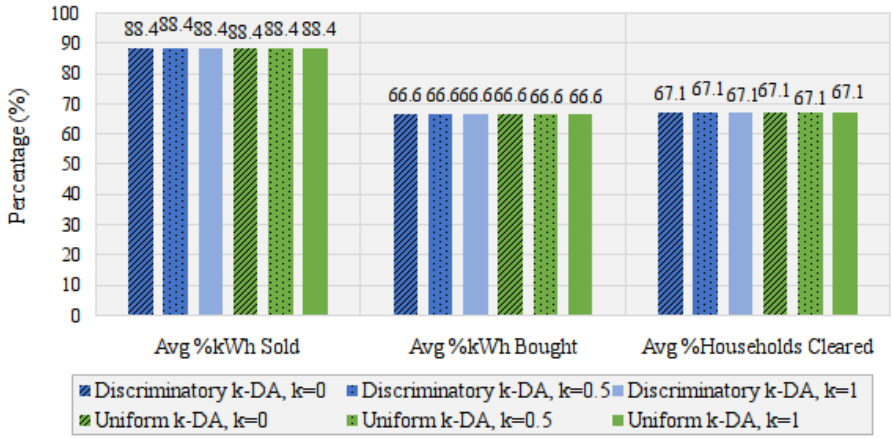

Fig. 14. Ideal market performance at 50% PV penetration.

Fig. 14 shows the ideal market performance at 50% PV penetration. Note that the average percentage of kWh sold decreased from 100% in the ideal 30% PV penetration scenario to 88.4% due to excess PV output from the microgrid. There is a surplus of

supply – thus only 88.4% can be sold within the microgrid to fulfill buyer demand. Due to excess supply and less buyer demand, fulfilment of buyer demand increased from 38.4% to 66.6%. At 50% PV penetration, this ideal scenario can completely satisfy energy needs of, on average, 67.1% of all households in the microgrid.

4.3.2.1 Random Bidding Strategy

Results in Fig. 15 with participants employing the random bidding strategy in a 50-prosumer microgrid indicate the same generality as a 30-prosumer microgrid (Case I) with participants employing the same strategy. Discriminatory *k*-DA leads to the same average percentage of households whose orders are completely filled as uniform *k*-DA. Similarly, all three metrics indicate same results for both mechanisms regardless of *k* values. However, there is less average percentage of kWh sold when compared to the 76.2% in Case I scenario 4.3.1.1 (random bidding strategy, 30% PV penetration). This is due to the market having excess supply, more than enough to fulfill microgrid demands in the hours of ~08:30 to ~13:30. In turn, there is a higher percentage of kWh bought because there is no longer a shortage of supply as in Case I scenario 4.3.1.1.

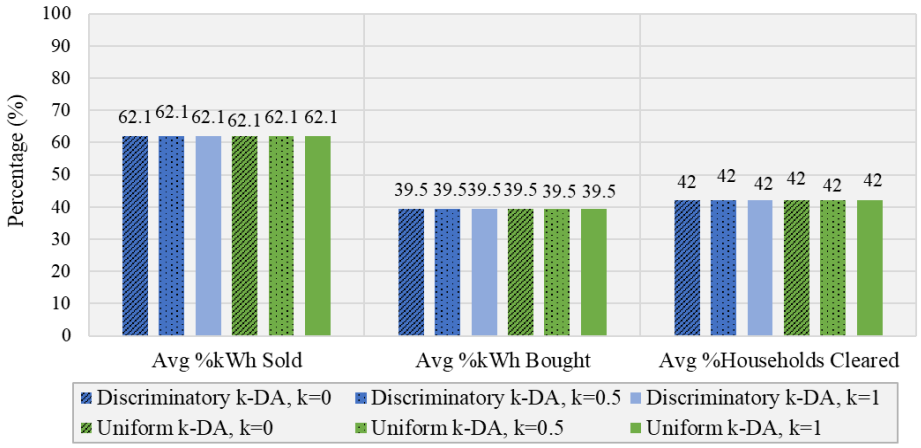

Fig. 15. Performance comparison for random bidding strategy at 50% PV penetration.

4.3.2.2 Preference Factor Bidding Strategy

In line with scenario 4.3.1.2 (preference factor bidding strategy at 30% PV penetration), results in Fig. 16 show significantly lower performance when compared to other bidding strategies at the same level of PV penetration. In addition, the trend of decreasing average percentage of kWh sold and increasing average percentage of kWh bought follow that of random bidding strategy. This is again due to the microgrid having excess PV supply; there is no longer a shortage of supply as in Case I 30% PV penetration scenarios.

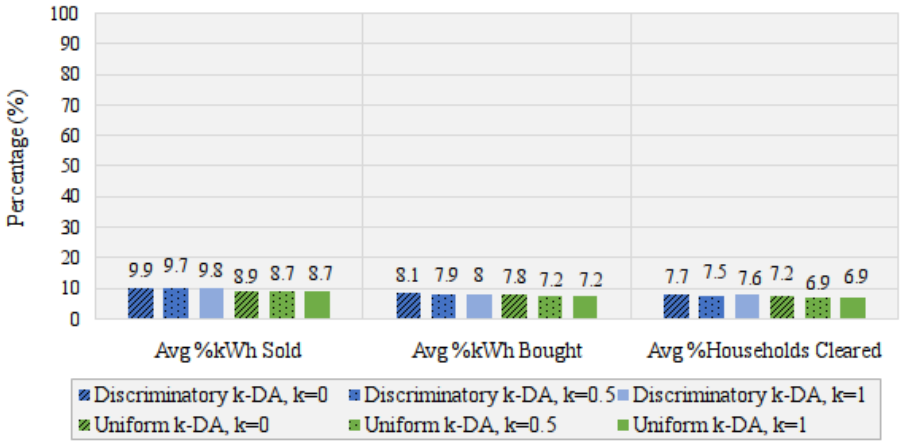

Fig. 16. Performance comparison for preference factor bidding strategy at 50% PV penetration.

4.3.2.3 Price-Only Game-Theoretic Bidding Strategy

Fig. 17 shows the performance when participants employ the price-only game-theoretic approach in a microgrid with 50% PV penetration. Results reveal that the performance of this bidding strategy is again close to ideal. Economic efficiencies are comparable for both auction mechanisms with the exception of discriminatory *k*-DA when *k*=0. Such can be attributed to low transaction volumes in this scenario.

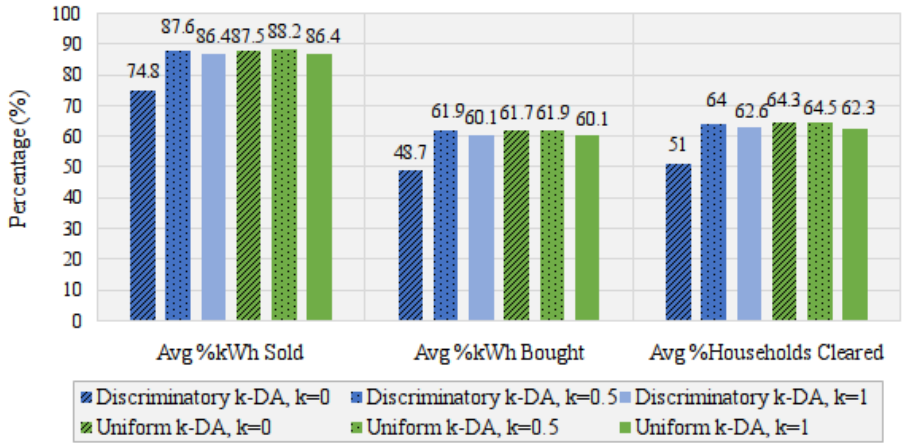

Fig. 17. Performance comparison for price-only game theory strategy at 50% PV penetration.

4.3.2.4 Supply-Demand Game-Theoretic Bidding Strategy

Fig. 18 shows the performance of the game-theoretic strategy when a supply-demand method is used to determine payoffs. There is no longer a decreasing trend in performance as *k* value increases due to excess supply in the microgrid. Thus at 50% PV penetration, the microgrid is a buyers' market. Such is evident when comparing Table 10 (supply-demand game, 30% PV penetration) and Table 11 (supply-demand game, 50% PV penetration): market prices for each hour decreased regardless of the auction mechanism. In addition from Table 11, it can be observed that market rates decrease during the hours of excess supply (from ~08:30 to ~13:30 in Fig. 13). However outside of those hours when there is more demand than supply, market rates increase.

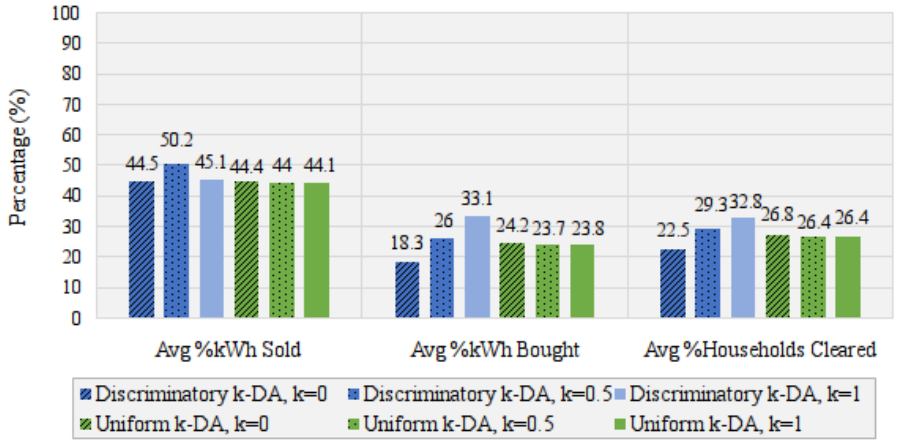

Fig. 18. Performance comparison for supply-demand game theory strategy at 50% PV penetration.

4.3.3 Case III: 70% PV Penetration

Fig. 19 illustrates the load and PV generation profiles for a microgrid of 30 consumers and 70 prosumers. At 70% PV penetration, the total PV capacity in this microgrid is 640.9kW; peak PV output is ~530kW at around 12:00. As in Case II, there is an excess of PV energy from the microgrid between ~07:30 to 15:00 even after self-consumption. Note that there is more demand from the sellers due to higher ratio of prosumers to consumers. However, the total microgrid demand profile maintains the same and is consistent with that of Case I and Case II.

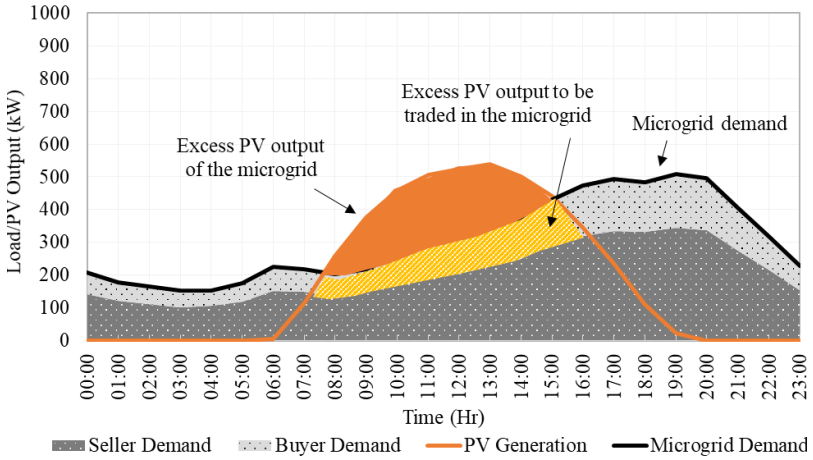

Fig. 19. Microgrid supply vs demand at 70% PV penetration.

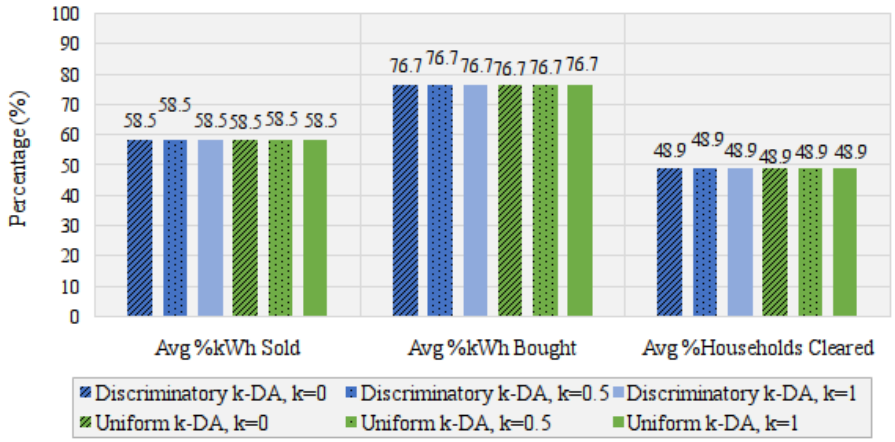

Fig. 20. Ideal market performance at 70% PV penetration.

Fig. 20 shows the ideal market performance at 70% PV penetration. Average percentage of kWh sold further decreased from Case II (88.4% to 58.5%) due to even more excess PV output from the microgrid. Average percentage of kWh bought increased from 66.6% to 76.7% due to less total buyer demand. At 70% PV penetration, this ideal market scenario can completely satisfy energy needs of, on average, 48.9% of all households in the microgrid. This decrease from Case II (67.1% to 48.9%) can be attributed to the higher number of prosumers who are not able to completely sell their excess energy within the microgrid.

4.3.3.1 Random Bidding Strategy

Results in Fig. 21 indicate the same outcome pertaining to discriminatory and uniform *k*-DA as in Cases I and II. In line with more excess PV generation, there is a lower average percentage of kWh sold. However, there is a higher average percentage of kWh bought as there is less consumer demand with excess supply.

For all three levels of PV penetration with agents employing random bidding strategies, discriminatory *k*-DA performs equivalently as uniform *k*-DA with respect to

the three defined economic efficiency indices: average percentage of kWh sold/bought and average percentage of households cleared.

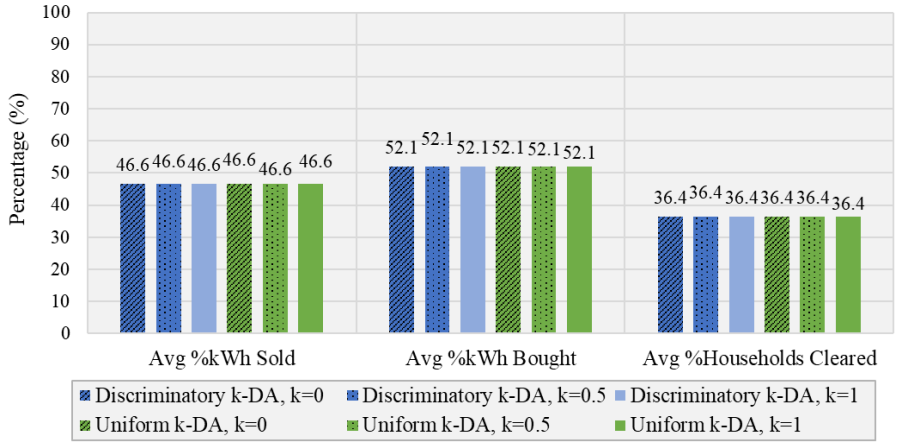

Fig. 21. Performance comparison for random bidding strategy at 70% PV penetration.

4.3.3.2 Preference Factor Bidding Strategy

Fig. 22 presents the trading performance result at 70% PV penetration. The average percentage of kWh sold is lower than that of 30% and 50% PV penetration. Such result is consistent with the two other bidding strategies – there is more excess supply from prosumers to meet decreasing consumer load demands. Despite so, the preference factor bidding strategy still results in the lowest performing bidding strategy as most buyers seek a discount from market rates while most buyers seek a premium from market rates. Thus, transactions presented in Fig. 22 result from participants who are willing to sacrifice maximization of personal financial gain to support green energy production as well as the local community.

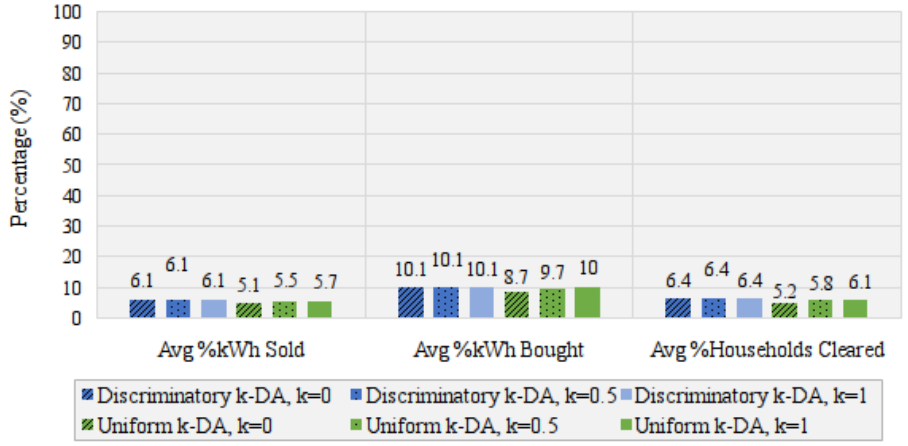

Fig. 22. Performance comparison for preference factor bidding strategy at 70% PV penetration.

4.3.3.3 Price-Only Game-Theoretic Bidding Strategy

Fig. 23 shows the performance comparison for the price-only game at 70% PV penetration. Once again, performance is near ideal. With this approach, the amount of transactions between prosumers and consumers is significantly higher than that of the preference factor bidding strategy or random bidding strategy, regardless of the level of PV penetration. In addition, the overall performance of discriminatory *k*-DA is comparable to that uniform *k*-DA, regardless of *k* value.

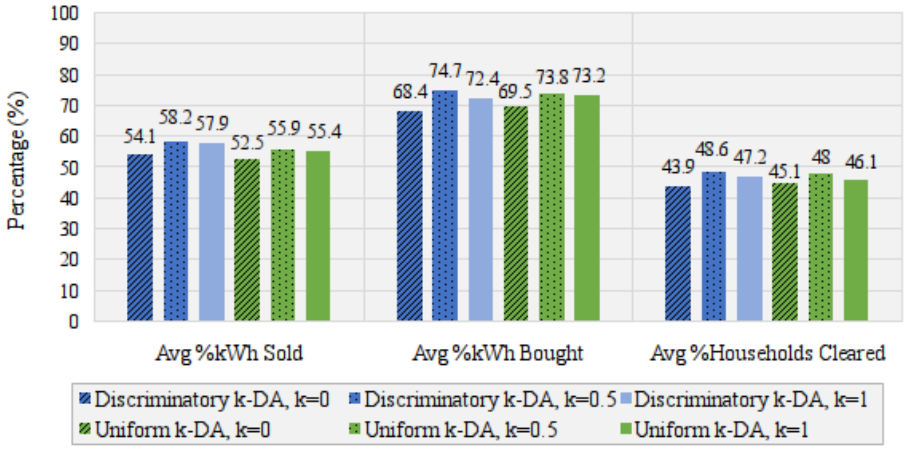

Fig. 23. Performance comparison for price-only game theory strategy at 70% PV penetration.

4.3.3.4 Supply-Demand Game-Theoretic Bidding Strategy

Exhibited in Fig. 24, the supply-demand payoff approach results in significantly worse economic efficiencies than case 4.3.2.4 (supply-demand game, 50% PV penetration). At 70% PV penetration, there is more supply than demand. This scenario is thus a buyers' market, where the low performance can be attributed to buyers who maintain low bids. The effect is further compounded by the *k* value in the discriminatory mechanism. With even more excess supply than 50% PV penetration, market prices for each hour are observed to have decreased from Table 12 to Table 14, regardless of auction mechanism. Similar to case 4.3.2.4 (supply-demand game, 50% PV penetration), it can be observed from Table 14 that market rates decrease during the hours of excess supply (from ~07:30 to 15:00 in Fig. 19). However outside of those hours when there is more demand than supply, market rates increase.

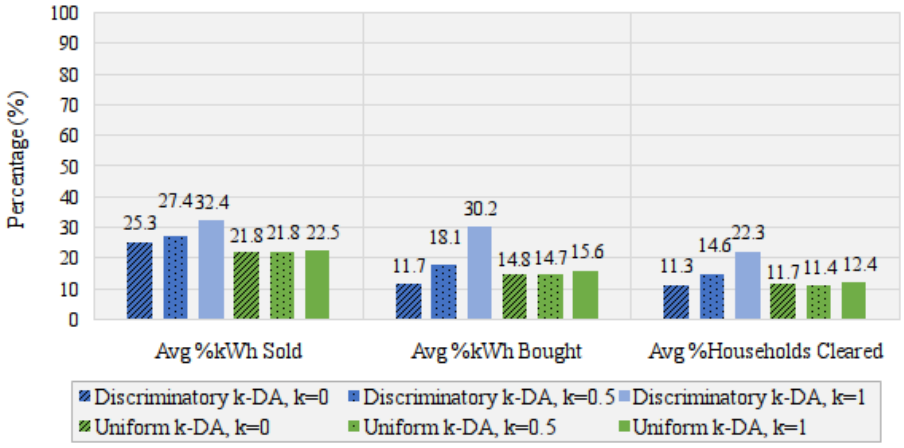

Fig. 24. Performance comparison for supply-demand game theory strategy at 70% PV penetration.

Regardless of PV penetration and auction mechanism, it is clear that the price-only game-theoretic bidding strategy results in near-ideal performance for all three metrics: average percentage of kWh sold/bought and average percentage of households

cleared. However when supply and demand are taken into account during the price determination process, performance drops significantly regardless of PV penetration or auction mechanism. Additionally, it can be observed that discriminatory *k*-DA is more sensitive to market conditions and level of PV penetration, even though it may perform better than uniform *k*-DA depending on its *k* value.

4.4 Observations

Considered in this simulation are extreme scenarios where all participants within a microgrid place bids using the same strategies. In a realistic market, participants would employ different strategies, thus leading to results that lie within the findings presented in this thesis. However, it is evident that the preference factor bidding strategy results in the lowest performance as participants are modeled to seek personal gain solely from previous-hour market rates without other considerations. Bidding with the supply-demand game-theoretic approach results in slightly better performance due to participants considering the best strategy to outbid other participants. However because market supply and demand are taken into account, buyers from a buyers' market and sellers from a sellers' market may maintain their low and high bids/asks, respectively. Surprisingly, this results in lower performance in contrast to all participants bidding at uniformly random prices. Still, the best performing strategy is the price-only game-theoretic strategy. This approach results in near-ideal performance in supplying consumer energy needs, selling excess prosumer energy generation, and fulfilling orders within the microgrid market.

The second observation pertains to the economic efficiency of the supply-demand game across various PV penetration levels. From the progression of 30% PV penetration

to 50% PV penetration, all other bidding strategies resulted in lower average percentage of kWh sold and higher average percentage of kWh bought. Such follows the same trend in ideal situations where all participants bid with the same price. However for the supply-demand game, economic efficiencies increased for both average percentage of kWh sold and average percentage of kWh bought. Additionally from the progression of 50% PV penetration to 70% PV penetration, all other bidding strategies resulted in even lower average percentage of kWh sold and higher average percentage of kWh bought. However, performance of the two respective metrics decreased for the supply-demand game. Such peculiar behavior is attributed to the participants' knowledge of market supply and demand. Economic efficiencies no longer depend on bid/ask prices, but also on quantities available/needed in the market. Table 8 summarizes the market information for the supply-demand game for discriminatory *k*-DA when k=0 and P_{seed}=7.82¢/kWh. Clearly, 50% PV penetration results in the highest average percentage of fulfilled market orders within the microgrid. Such occurs because market supply is more closely matched with market demand than any other PV penetration levels.

Table 8. Market data for supply-demand game (discriminatory *k*-DA, k=0, P_{seed}=7.82¢/kWh).

PV Penetration	Avg %Households Cleared	Traded kWh	Supplied kWh	Demanded kWh	Average Market Price
30%	19.6%	268.1	819.9	2677.9	11.01¢/kWh
50%	22.5%	396.9	1393.2	1914.6	7.34¢/kWh
70%	11.3%	237	1957.3	1168.1	6.29¢/kWh

The reflected candlestick charts of hourly market prices for the different levels of PV penetration are shown in Fig. 25. At 30% PV penetration, demand is always greater than supply. Thus, market prices rise. At 50% PV penetration, market rates fall when there is excess supply and rise when there is greater demand in early morning and

afternoon. At 70% PV penetration, market rates fall even further during the period of excess PV output from the microgrid.

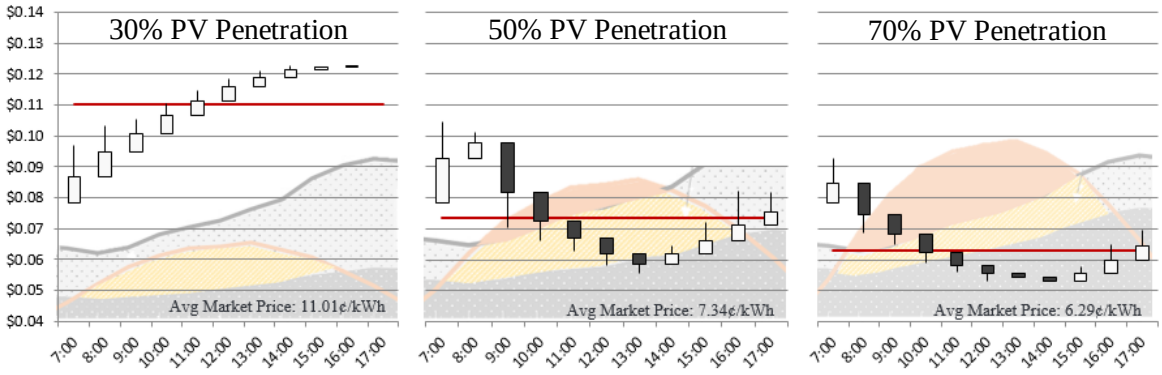

Fig. 25. Hourly market rates for supply-demand game (discriminatory *k*-DA, *k*=0, P_{seed}=7.82¢/kWh).

Additionally, an intriguing phenomenon can be observed in the price-only game: consistent throughout all three PV penetration levels, the lowest economic efficiency results when *k*=0. Logically, such occurrence is attributed to the low number of transactions due to a mismatch between buyer bids and seller asks. Upon further investigation, Table 9, Table 11, and Table 13 reveal an interesting connection: all market rates fall within the lower and upper quartile of the sellers' marginal costs ($0.0679/kWh and $0.0841/kWh, respectively). Consequently, the number of transactions decrease as market rates approach marginal costs. Such also explains why certain hours of the supply-demand game at 30% PV penetration when *k*=1 resulted in zero trades. Reported in Table 10, market rates quickly approach the mean of the buyers' marginal cost – $0.1234/kWh.

CHAPTER 5. CONCLUSION

An hour-ahead P2P energy trading network based on the Hyperledger Fabric blockchain is constructed. In addition, a comparative analysis of auction mechanisms that can facilitate a transactive energy market is explored under three levels of PV penetration. A microgrid of 100 homes with 30%, 50%, and 70% PV penetration levels is simulated through a custom developed framework against four participant bidding strategies. Results indicate that regardless of PV penetration and employed bidding strategies, discriminatory *k*-DA can outperform uniform *k*-DA in all three performance metrics – average percentage of kWh sold, average percentage of kWh bought, and average percentage of households cleared. Despite so, discriminatory *k*-DA is more sensitive to market conditions than uniform *k*-DA. When participants employ a preference factor bidding strategy, performance with respect to all three metrics is the lowest of the four strategies. Such makes sense as the strategy models participant behavior to seek prices better than the previous-hour market rate. In this situation, sellers tend to seek higher returns than the market price while buyers tend to seek lower costs than the market price. If all participants seek better-than-market rates, all three evaluation metrics would result in 0% as there would be no transactions in the market. However, such is not the case in a realistic market as some participants may be willing to transact at slightly inferior rates to benefit the local community and support the production of green energy. Bidding with the supply-demand game-theoretic method results in slightly higher performance due to participants attempting to outbid other participants rather than focusing on individual gain. Despite so, this strategy underperforms by a significant margin when compared to bidding at uniformly random prices. The best performing

strategy is the price-only game theoretic approach. This method results in near-ideal economic efficiency with respect to all three metrics: supplying consumer energy needs, selling excess prosumer energy generation, and fulfilling orders within the microgrid market. Such is due to participants attempting to outbid their peers to offer the best prices regardless of market condition.

Thus, potential market applicability of P2P energy trading may be targeted towards microgrids at locations where net metering or premium feed-in tariffs are *unavailable*. At locations where net metering is *available*, there is little incentive for monetary-driven prosumers to participate in P2P energy trading as they cannot financially gain more than participating in the program, which offers credits at full retail rate. Such also applies to locations where premium feed-in tariffs are offered. Thus, there must exist a high differential between the location's average cost of electricity and its feed-in tariff at avoided cost rate, in order for the TE market to be effective. Otherwise, there is no incentive to set up the infrastructure to support such market. When such margin between the two costs exist, prosumers are able to enjoy higher-than-avoided-cost returns while consumers are able to enjoy lower average costs of electricity, at the added benefit of supporting locally produced green energy. In addition, such TE market keeps monetary circulation and economic activity with the local community.

Through conducted simulations, the author noticed that the results of game-theoretic bidding strategies are sensitive to each agent's utility function as well as payoff determination method. Thus, detailed studies of consumer/prosumer behavior can be conducted and modeled for future work. In addition, more complex ordering rules may be incorporated, such as prioritizing prosumers who generate higher quality of electricity or

prioritizing low-income homeowners in need. Future work may also be expanded to include dynamic auction mechanisms where the smart contract adapts to varying supplies and demands in order to balance the P2P energy trading market. This work may further be extended to support various DERs, alternative fuel exchanges, as well as other emerging economies.

APPENDIX A. ADDITIONAL SIMULATION RESULTS

A.1 Case I: 30% PV Penetration

A.1.1 Price-Only Game-Theoretic Bidding Strategy

Table 9. Market price log for price-only game at 30% PV penetration ($/kWh).

	Discriminatory *k*-DA			**Uniform *k*-DA**		
Time	***k*=0**	***k*=0.5**	***k*=1**	***k*=0**	***k*=0.5**	***k*=1**
0:00	-	-	-	-	-	-
1:00	-	-	-	-	-	-
2:00	-	-	-	-	-	-
3:00	-	-	-	-	-	-
4:00	-	-	-	-	-	-
5:00	-	-	-	-	-	-
6:00	-	-	-	-	-	-
7:00	0.0690	0.0915	0.1140	0.0778	0.0922	0.1065
8:00	0.0713	0.0991	0.1194	0.0886	0.1054	0.1117
9:00	0.0738	0.1014	0.1199	0.1009	0.1082	0.1135
10:00	0.0736	0.1013	0.1202	0.1009	0.1094	0.1135
11:00	0.0742	0.1011	0.1205	0.1022	0.1104	0.1135
12:00	0.0740	0.1015	0.1207	0.1022	0.1114	0.1135
13:00	0.0758	0.1021	0.1210	0.1022	0.1123	0.1135
14:00	0.0756	0.1034	0.1213	0.1022	0.1125	0.1135
15:00	0.0762	0.1059	0.1218	0.1022	0.1133	0.1137
16:00	0.0769	0.1084	0.1223	0.1104	0.1141	0.1149
17:00	0.0837	0.1110	0.1233	0.1098	0.1177	0.1222
18:00	-	-	-	-	-	-
19:00	-	-	-	-	-	-
20:00	-	-	-	-	-	-
21:00	-	-	-	-	-	-
22:00	-	-	-	-	-	-
23:00	-	-	-	-	-	-

A.1.2 Supply-Demand Game-Theoretic Bidding Strategy

Table 10. Market price log for supply-demand game at 30% PV penetration ($/kWh).

	Discriminatory *k*-DA			**Uniform *k*-DA**		
Time	***k*=0**	***k*=0.5**	***k*=1**	***k*=0**	***k*=0.5**	***k*=1**
0:00	-	-	-	-	-	-
1:00	-	-	-	-	-	-
2:00	-	-	-	-	-	-
3:00	-	-	-	-	-	-
4:00	-	-	-	-	-	-
5:00	-	-	-	-	-	-
6:00	-	-	-	-	-	-
7:00	0.0869	0.0982	0.1095	0.0970	0.1021	0.1071
8:00	0.0948	0.1115	0.1212	0.1096	0.1153	0.1167
9:00	0.1006	0.1179	0.1231	0.1177	0.1211	0.1215
10:00	0.1066	0.1217	-	0.1217	0.1227	0.1234
11:00	0.1114	0.1230	0.1234	0.1225	-	-
12:00	0.1158	-	-	0.1233	0.1233	0.1234
13:00	0.1190	0.1207	0.1224	-	-	-
14:00	0.1213	0.1224	0.1233	0.1232	0.1233	0.1233
15:00	0.1221	0.1233	-	-	-	-
16:00	0.1229	-	-	-	-	-
17:00	-	-	-	-	-	-
18:00	-	-	-	-	-	-
19:00	-	-	-	-	-	-
20:00	-	-	-	-	-	-
21:00	-	-	-	-	-	-
22:00	-	-	-	-	-	-
23:00	-	-	-	-	-	-

A.2 Case II: 50% PV Penetration

A.2.1 Price-Only Game-Theoretic Bidding Strategy

Table 11. Market price log for price-only game at 50% PV penetration ($/kWh).

	Discriminatory *k*-DA			**Uniform *k*-DA**		
Time	***k*=0**	***k*=0.5**	***k*=1**	***k*=0**	***k*=0.5**	***k*=1**
0:00	-	-	-	-	-	-
1:00	-	-	-	-	-	-
2:00	-	-	-	-	-	-
3:00	-	-	-	-	-	-
4:00	-	-	-	-	-	-
5:00	-	-	-	-	-	-
6:00	-	-	-	-	-	-
7:00	0.0740	0.0940	0.1140	0.1022	0.1032	0.1042
8:00	0.0738	0.0975	0.1167	0.1022	0.1032	0.1042
9:00	0.0716	0.0967	0.1171	0.1022	0.1032	0.1042
10:00	0.0700	0.0958	0.1177	0.1022	0.1030	0.1042
11:00	0.0693	0.0953	0.1179	0.1022	0.1030	0.1042
12:00	0.0688	0.0952	0.1179	0.1022	0.1030	0.1042
13:00	0.0688	0.0966	0.1181	0.1017	0.1030	0.1042
14:00	0.0695	0.0985	0.1186	0.1017	0.1030	0.1042
15:00	0.0714	0.1024	0.1193	0.1017	0.1030	0.1042
16:00	0.0740	0.1065	0.1204	0.1019	0.1044	0.1053
17:00	0.0735	0.1089	0.1230	0.1014	0.1121	0.1190
18:00	-	-	-	-	-	-
19:00	-	-	-	-	-	-
20:00	-	-	-	-	-	-
21:00	-	-	-	-	-	-
22:00	-	-	-	-	-	-
23:00	-	-	-	-	-	-

A.2.2 Supply-Demand Game-Theoretic Bidding Strategy

Table 12. Market price log for supply-demand game at 50% PV penetration ($/kWh).

	Discriminatory *k*-DA			**Uniform *k*-DA**		
Time	***k*=0**	***k*=0.5**	***k*=1**	***k*=0**	***k*=0.5**	***k*=1**
0:00	-	-	-	-	-	-
1:00	-	-	-	-	-	-
2:00	-	-	-	-	-	-
3:00	-	-	-	-	-	-
4:00	-	-	-	-	-	-
5:00	-	-	-	-	-	-
6:00	-	-	-	-	-	-
7:00	0.0927	0.1007	0.1086	0.0970	0.1002	0.1033
8:00	0.0976	0.1113	0.1189	0.1056	0.1091	0.1117
9:00	0.0818	0.0971	0.1126	0.0954	0.0989	0.1016
10:00	0.0725	0.0875	0.1074	0.0872	0.0913	0.0928
11:00	0.0672	0.0800	0.1027	0.0821	0.0859	0.0878
12:00	0.0621	0.0748	0.0981	0.0788	0.0817	0.0831
13:00	0.0587	0.0714	0.0946	0.0756	0.0786	0.0802
14:00	0.0619	0.0810	0.1095	0.0823	0.0863	0.0888
15:00	0.0663	0.0945	0.1209	0.0911	0.0957	0.0986
16:00	0.0713	0.1079	0.1233	0.1008	0.1063	0.1098
17:00	0.0755	0.1173	-	0.1153	0.1179	0.1223
18:00	-	-	-	-	-	-
19:00	-	-	-	-	-	-
20:00	-	-	-	-	-	-
21:00	-	-	-	-	-	-
22:00	-	-	-	-	-	-
23:00	-	-	-	-	-	-

A.3 Case III: 70% PV Penetration

A.3.1 Price-Only Game-Theoretic Bidding Strategy

Table 13. Market price log for price-only game at 70% PV penetration ($/kWh).

	Discriminatory *k*-DA			**Uniform *k*-DA**		
Time	***k*=0**	***k*=0.5**	***k*=1**	***k*=0**	***k*=0.5**	***k*=1**
0:00	-	-	-	-	-	-
1:00	-	-	-	-	-	-
2:00	-	-	-	-	-	-
3:00	-	-	-	-	-	-
4:00	-	-	-	-	-	-
5:00	-	-	-	-	-	-
6:00	-	-	-	-	-	-
7:00	0.0772	0.0956	0.1140	0.0860	0.0908	0.0955
8:00	0.0730	0.0946	0.1160	0.0814	0.0874	0.0936
9:00	0.0693	0.0917	0.1154	0.0803	0.0848	0.0936
10:00	0.0670	0.0896	0.1159	0.0792	0.0827	0.0936
11:00	0.0654	0.0875	0.1159	0.0788	0.0823	0.0930
12:00	0.0638	0.0861	0.1167	0.0784	0.0824	0.0930
13:00	0.0635	0.0856	0.1160	0.0780	0.0825	0.0925
14:00	0.0636	0.0857	0.1162	0.0780	0.0826	0.0925
15:00	0.0648	0.0887	0.1174	0.0780	0.0832	0.0920
16:00	0.0682	0.0966	0.1186	0.0790	0.0840	0.0920
17:00	0.0751	0.1060	0.1233	0.0869	0.0974	0.1102
18:00	-	-	-	-	-	-
19:00	-	-	-	-	-	-
20:00	-	-	-	-	-	-
21:00	-	-	-	-	-	-
22:00	-	-	-	-	-	-
23:00	-	-	-	-	-	-

A.3.2 Supply-Demand Game-Theoretic Bidding Strategy

Table 14. Market price log for supply-demand game at 70% PV penetration ($/kWh).

	Discriminatory *k*-DA			**Uniform *k*-DA**		
Time	***k*=0**	***k*=0.5**	***k*=1**	***k*=0**	***k*=0.5**	***k*=1**
0:00	-	-	-	-	-	-
1:00	-	-	-	-	-	-
2:00	-	-	-	-	-	-
3:00	-	-	-	-	-	-
4:00	-	-	-	-	-	-
5:00	-	-	-	-	-	-
6:00	-	-	-	-	-	-
7:00	0.0849	0.0907	0.0965	0.0925	0.0930	0.0934
8:00	0.0748	0.0825	0.0931	0.0829	0.0834	0.0837
9:00	0.0682	0.0759	0.0892	0.0757	0.0767	0.0774
10:00	0.0625	0.0714	0.0857	0.0726	0.0738	0.0747
11:00	0.0582	0.0677	0.0830	0.0697	0.0710	0.0721
12:00	0.0556	0.0643	0.0803	0.0669	0.0683	0.0696
13:00	0.0543	0.0616	0.0779	0.0646	0.0660	0.0672
14:00	0.0530	0.0596	0.0761	0.0624	0.0640	0.0653
15:00	0.0557	0.0658	0.0880	0.0660	0.0679	0.0694
16:00	0.0599	0.0752	0.1064	0.0709	0.0730	0.0746
17:00	0.0643	0.0867	0.1202	0.0824	0.0860	0.0891
18:00	-	-	-	-	-	-
19:00	-	-	-	-	-	-
20:00	-	-	-	-	-	-
21:00	-	-	-	-	-	-
22:00	-	-	-	-	-	-
23:00	-	-	-	-	-	-

REFERENCES

[1] Utility Dive, “2016 STATE OF THE ELECTRIC UTILITY SURVEY.” [Online]. Available: https://s3.amazonaws.com/dive_assets/rlpsys/state_of_electric_utility_2016.pdf. [Accessed: 02-Nov-2018].

[2] "Form EIA-861M detailed data – Net Metering", Electricity, 2018. [Online]. Available: https://www.eia.gov/electricity/data/eia861m/xls/net_metering2018.xlsx. [Accessed: 04-Nov-2018].

[3] N. (DAV-SEAC), "The Open PV Project", The Open PV Project, 2018. [Online]. Available: https://openpv.nrel.gov/. [Accessed: 04-Nov-2018].

[4] "Form EIA-861M detailed data – Small Scale PV", Electricity, 2018. [Online]. Available: https://www.eia.gov/electricity/data/eia861m/xls/small_scale_solar_2018.xlsx. [Accessed: 04-Nov-2018].

[5] "Grid-Connected Renewable Energy Systems", U.S. Department of Energy, 2018. [Online]. Available: https://www.energy.gov/energysaver/grid-connected-renewable-energy-systems. [Accessed: 04-Nov-2018].

[6] "Energy Policy Act of 2005: Summary and Analysis of Enacted Provisions", Circle of Blue, 2018. [Online]. Available: https://www.circleofblue.org/wp-content/uploads/2010/08/CRS-Summary-of-Energy-Policy-Act-of-2005.pdf. [Accessed: 28- Nov- 2018].

[7] "ENERGY POLICY ACT OF 2005", U.S. GOVERNMENT PUBLISHING OFFICE, 2018. [Online]. Available: https://www.gpo.gov/fdsys/pkg/PLAW-109publ58/pdf/PLAW-109publ58.pdf. [Accessed: 28- Nov- 2018].

[8] "Schedule 1 Residential Service", Dominion Energy, 2018. [Online]. Available: https://www.dominionenergy.com/library/domcom/media/home-and-small-business/rates-and-regulation/residential-rates/virginia/schedule-1.pdf. [Accessed: 28- Nov- 2018].

[9] "How many solar panels do you need to power your house?", Solar Power Rocks, 2018. [Online]. Available: https://www.solarpowerrocks.com/square-feet-solar-roof/. [Accessed: 28- Nov- 2018].

[10] "Consumers Energy - Experimental Advanced Renewable Program", DSIRE, 2018. [Online]. Available: http://programs.dsireusa.org/system/program/detail/5752. [Accessed: 28- Nov- 2018].

[11] "November 2009", Electric Power Monthly, 2018. [Online]. Available: https://www.eia.gov/electricity/monthly/archive/pdf/02260911.pdf. [Accessed: 28- Nov- 2018].

[12] "Net Metering", DSIRE, 2018. [Online]. Available: http://programs.dsireusa.org/system/program/detail/342. [Accessed: 28- Nov- 2018].

[13] "September 2018", Electric Power Monthly, 2018. [Online]. Available: https://www.eia.gov/electricity/monthly/epm_table_grapher.php?t=epmt_5_6_a. [Accessed: 28- Nov- 2018].

[14] "Electricity 2018", Wholesale Electricity and Natural Gas Market Data, 2018. [Online]. Available: https://www.eia.gov/electricity/wholesale/xls/ice_electric-2018.xlsx. [Accessed: 28- Nov- 2018].

[15] "The Solar Net Metering Controversy: Who Pays For Energy Subsidies?", Forbes, 2018. [Online]. Available: https://www.forbes.com/sites/uhenergy/2016/03/16/the-solar-net-metering-controversy-who-pays-for-energy-subsidies/#bc534186fd29. [Accessed: 28- Nov- 2018].

[16] "Solar Cost-Benefit Studies", SEIA, 2018. [Online]. Available: https://www.seia.org/initiatives/solar-cost-benefit-studies. [Accessed: 28- Nov- 2018].

[17] M. Saha, "Rooftop solar: Net metering is a net benefit", Brookings, 2018. [Online]. Available: https://www.brookings.edu/research/rooftop-solar-net-metering-is-a-net-benefit/. [Accessed: 28- Nov- 2018].

[18] "The Future of Peer-to-Peer Energy Trading", Oxford Martin School, 2018. [Online]. Available: https://www.oxfordmartin.ox.ac.uk/opinion/view/394. [Accessed: 28- Nov- 2018].

[19] J. Murkin, R. Chitchyan and A. Byrne, "Enabling peer-to-peer electricity trading", Proceedings of ICT for Sustainability 2016, 2016.

[20] M. Andoni, V. Robu, D. Flynn, S. Abram, D. Geach, D. Jenkins, P. McCallum and A. Peacock, "Blockchain technology in the energy sector: A systematic review of challenges and opportunities", Renewable and Sustainable Energy Reviews, vol. 100, pp. 143-174, 2018.

[21] Z. Zheng, S. Xie, H. Dai, X. Chen and H. Wang, "An Overview of Blockchain Technology: Architecture, Consensus, and Future Trends", 2017 IEEE International Congress on Big Data (BigData Congress), 2017.
[22] X. Xu, I. Weber, M. Staples, L. Zhu, J. Bosch, L. Bass, C. Pautasso and P. Rimba, "A Taxonomy of Blockchain-Based Systems for Architecture Design", 2017 IEEE International Conference on Software Architecture (ICSA), 2017.
[23] L. Lamport, R. Shostak and M. Pease, "The Byzantine Generals Problem," *ACM Transactions on Programming Languages and Systems*, vol. 4, no. 3, pp. 382-401, 1982
[24] M. Castro and B. Liskov, "Practical byzantine fault tolerance", OSDI '99 Proceedings of the third symposium on Operating systems design and implementation, pp. 173-186, 1999.
[25] A. Zohar, "Bitcoin: under the hood," *Communications of the ACM*, vol. 58, no. 9, pp. 104-113, 2015
[26] J. A. Kroll, I. C. Davey, and E. W. Felten, "The economics of bitcoin mining, or bitcoin in the presence of adversaries," 2013.
[27] I. Eyal and E. Sirer, "Majority is not enough", Communications of the ACM, vol. 61, no. 7, pp. 95-102, 2018.
[28] A. Baliga, "Understanding Blockchain Consensus Models" [Online]. Available: https://pdfs.semanticscholar.org/da8a/37b10bc1521a4d3de925d7ebc44bb606d740.pdf. [Accessed: 02-Nov-2018].
[29] Z. Zheng, S. Xie, H. Dai, X. Chen and H. Wang, "Blockchain challenges and opportunities: a survey", International Journal of Web and Grid Services, vol. 14, no. 4, p. 352, 2018.
[30] "Ethereum White Paper", GitHub, 2018. [Online]. Available: https://github.com/ethereum/wiki/wiki/White-Paper. [Accessed: 28- Nov- 2018].
[31] "Ethereum Proof of Stake FAQs", GitHub, 2018. [Online]. Available: https://github.com/ethereum/wiki/wiki/Proof-of-Stake-FAQs. [Accessed: 28- Nov- 2018].
[32] "Hyperledger Architecture, Volume 1", Hyperledger, 2018. [Online]. Available: https://www.hyperledger.org/wp-content/uploads/2017/08/Hyperledger_Arch_WG_Paper_1_Consensus.pdf. [Accessed: 28- Nov- 2018].
[33] "Hyperledger Fabric Documentation", Hyperledger, 2018. [Online]. Available: https://media.readthedocs.org/pdf/hyperledger-fabric/latest/hyperledger-fabric.pdf. [Accessed: 28- Nov- 2018].
[34] M. Valenta and P. Sandner, "Comparison of Ethereum, Hyperledger Fabric and Corda", Frankfurt School, 2017. [Online]. Available: http://explore-ip.com/2017_Comparison-of-Ethereum-Hyperledger-Corda.pdf. [Accessed: 28- Nov- 2018].
[35] "Brooklyn Microgrid," Brooklyn Microgrid. [Online]. Available: https://www.brooklyn.energy/. [Accessed: 02- Sep- 2018].
[36] "New York consumers turn homes into connected power stations to take on the energy giants," LO3 Energy. [Online]. Available: https://lo3energy.com/new-york-consumers-turn-homes-connected-power-stations-take-energy-giants/. [Accessed: 02- Sep- 2018].
[37] E. Mengelkamp, J. Gärttner, K. Rock, S. Kessler, L. Orsini and C. Weinhardt, "Designing microgrid energy markets", Applied Energy, vol. 210, pp. 870-880, 2018.
[38] "Latrobe Valley Microgrid Feasibility Study", Australian Renewable Energy Agency, 2018. [Online]. Available: https://arena.gov.au/projects/latrobe-valley-microgrid-feasibility-study/. [Accessed: 28- Nov- 2018].
[39] "uGrid", Power Ledger, 2018. [Online]. Available: https://www.powerledger.io/products/micro-grid. [Accessed: 28- Nov- 2018].
[40] "Power Ledger P2P Platform Goes Across the Meter with BCPG at T77 Precinct, Bangkok", Medium, 2018. [Online]. Available: https://medium.com/power-ledger/power-ledger-p2p-platform-goes-across-the-meter-with-bcpg-at-t77-precinct-bangkok-62df5aba3d0a. [Accessed: 28- Nov- 2018].
[41] "Power Ledger", Parliament of Western Australia, 2018. [Online]. Available: http://www.parliament.wa.gov.au/parliament/commit.nsf/(Evidence+Lookup+by+Com+ID)/0F1FF6F426E21DDF48258289001B1171/$file/20181008-+MAT-+Sub+No.+29A-+Power+Ledger-+public.pdf. [Accessed: 28- Nov- 2018].

[42] "Piclo Energy", Piclo Energy, 2018. [Online]. Available: https://piclo.energy/. [Accessed: 28- Nov- 2018].
[43] "sonnenCommunity", Sonnen Group, 2018. [Online]. Available: https://sonnengroup.com/sonnencommunity/. [Accessed: 28- Nov- 2018].
[44] M. Sabounchi and J. Wei, "Towards resilient networked microgrids: Blockchain-enabled peer-to-peer electricity trading mechanism," 2017 IEEE Conference on Energy Internet and Energy System Integration (EI2), Beijing, 2017, pp. 1-5.
[45] A. Hahn, R. Singh, C.-C. Liu, and S. Chen, "Smart contract-based campus demonstration of decentralized transactive energy auctions," 2017 IEEE Power & Energy Society Innovative Smart Grid Technologies Conference (ISGT), 2017.
[46] "GridWise Architecture Council," GridWise Architecture Council. [Online]. Available: www.gridwiseac.org. [Accessed: 04-Sep-2018].
[47] D. C. Parkes, "Classic Mechanism Design." Available: www.eecs.harvard.edu/~parkes/pubs/ch2.pdf. [Accessed: 04-Sep-2018].
[48] M. Babaioff and N. Nisan, "Concurrent auctions across the supply chain," Proceedings of the 3rd ACM conference on Electronic Commerce - EC 01, 2001.
[49] M. A. Satterthwaite and S. R. Williams, "Bilateral trade with the sealed bid k-double auction: Existence and efficiency," Journal of Economic Theory, vol. 48, no. 1, pp. 107–133, 1989.
[50] "Block", Bitcoin, 2018. [Online]. Available: https://en.bitcoin.it/wiki/Block. [Accessed: 28- Nov- 2018].
[51] "Ethereum Mining", Github, 2018. [Online]. Available: https://github.com/ethereum/wiki/wiki/Mining. [Accessed: 28- Nov- 2018].
[52] T. Dinh, J. Wang, G. Chen, R. Liu, B. Ooi and K. Tan, "BLOCKBENCH", Proceedings of the 2017 ACM International Conference on Management of Data - SIGMOD '17, 2017.
[53] J. Lin, M. Pipattanasomporn, and S. Rahman, "Comparative Analysis of Blockchain-based Smart Contracts for Solar Electricity Exchanges," *2019 IEEE Power & Energy Society Innovative Smart Grid Technologies Conference*, 2019
[54] "Q1/Q2 2018 Solar Industry Update", National Renewable Energy Laboratory, 2018. [Online]. Available: https://www.nrel.gov/docs/fy18osti/72036.pdf. [Accessed: 28- Nov- 2018].
[55] "Commercial and Residential Hourly Load Profiles for all TMY3 Locations in the United States," Open Energy Information. [Online]. Available: https://openei.org/doe-opendata/dataset/commercial-and-residential-hourly-load-profiles-for-all-tmy3-locations-in-the-united-states. [Accessed: 04-Sep-2018].
[56] US Department of Commerce and NOAA, "DCA Normals, Means, and Extremes," National Weather Service, 11-Jun-2015. [Online]. Available: www.weather.gov/lwx/dcanme. [Accessed: 04-Sep-2018].
[57] Virginia Tech Advanced Research Institute, "PV Generation Profile."
[58] I. Shapiro, "The Receptivity of Roofs for Solar Panels ", Taitem Engineering, 2018. [Online]. Available: https://www.taitem.com/wp-content/uploads/wsf2_887.pdf. [Accessed: 28- Nov- 2018].
[59] "Typical Roof Pitch," MyRooff.com. [Online]. Available: https://myrooff.com/standart-roof-pitch/. [Accessed: 22-Aug-2018].
[60] "5 Things to consider before you plan for a rooftop PV plant," Sustainability Outlook. [Online]. Available: http://www.sustainabilityoutlook.in/content/5-things-consider-you-plan-rooftop-pv-plant. [Accessed: 05-Sep-2018].